Environmental Toxicology and Chemistry, 2026, **00**, 1–25
https://doi.org/10.1093/etojnl/vgag143
Published: May 24, 2026
Original Article | **Environmental Toxicology**

Histopathology and transcriptomics in male zebrafish livers from a perfluorooctanesulfonic acid multigenerational exposure inform adverse outcome pathway development for liver steatosis

J. Erik Mylroie[1,2,*], Kurt A. Gust[1], Chad Blanksma[3], Alexander B. Lawrence[4,5], Allison Hoke[4], Ida Nela Crespo Rosales[4,6], Mitchell S. Wilbanks[1], Catherine S. C. Steward[7], Natàlia Garcia-Reyero[1], Aarti Gautam[4], Rasha Hammamieh[4], and David W. Moore[1]

[1]Environmental Laboratory, Engineer Research and Development Center, U.S. Army, Vicksburg, MS, United States
[2]Department of Biology, Millsaps College, Jackson, MS, United States
[3]Great Lakes Toxicology and Ecology Division, SpecPro Professional Services, Duluth, MN, United States
[4]Medical Readiness Systems Biology Branch, Center for Military Psychiatry and Neuroscience, Walter Reed Army Institute of Research, Silver Spring, MD, United States
[5]Army Educational Outreach Program, Gahanna, OH, United States
[6]Culmen International LLC, Arlington, VA, United States
[7]Bennett Aerospace, Cary, NC, United States
*Corresponding author: J. Erik Mylroie, Email: mylroje@millsaps.edu

Abstract

Poly- and perfluoroalkyl substance use in commercial products and industrial applications has resulted in widespread and persistent environmental contamination. Terrestrial and aquatic vertebrates accumulate poly- and perfluoroalkyl substances in liver tissue, potentially inducing hepatotoxicity. The present study investigated tissue-level and molecular effects in the livers of male zebrafish (*Danio rerio*) exposed for two generations to perfluorooctanesulfonic acid (PFOS). Histopathology and transcriptomic expression analysis (RNA sequencing) were performed for males exposed to PFOS at a control concentration (0 μg/L) and five nominal concentrations (0.1, 0.6, 3.2, 20, and 100 μg/L) through 180 days postfertilization in the parental (P) and first filial (F1) generations. Histopathological analysis indicated that the highest PFOS exposure (100 μg/L, nominal) caused significantly increased incidences of lipid-type hepatocellular vacuolation in P and F1 generations relative to controls with more prevalent and extensive effects in the F1 generation. The RNA sequencing analysis identified an increased number of transcripts significantly affected in PFOS exposures relative to controls in the F1 generation (955) versus the P generation (103), where both generations had most effects at the highest PFOS exposure (100 μg/L). Histopathological observations of disrupted lipid phenotypes in liver corresponded with transcriptomic identification of significantly enriched metabolic pathways underlying lipid metabolism, including cholesterol biosynthesis and the peroxisome proliferator–activated receptor (PPAR) pathway in both generations. To integrate these observations, an adverse outcome pathway was developed linking the molecular initiating event of a representative chemical stressor (PFOS) binding PPAR isoforms, binding-initiated interference of PPAR nuclear signaling to disrupted lipid metabolism, lipid accumulation in liver, and ultimately the liver steatosis adverse outcome.

Keywords zebrafish, perfluorooctanesulfonic acid, transcriptomics, adverse outcome pathway, histopathology

Introduction

Poly- and perfluoroalkyl substances (PFAS) are a large group of fluorinated compounds that have a variety of commercial and industrial applications, ranging from firefighting foams to nonstick coatings (Annunziato et al., 2020; DeWitt et al., 2019; Glüge et al., 2020). Exposure to PFAS can have negative effects on development, growth, reproduction, hepatic function, immune function, neurological function, and lipid metabolism in humans and other vertebrates (Agency for Toxic Substances and Disease Registry, 2021; Ankley et al., 2021; Bell et al., 2021; Boyd et al., 2022; Fragki et al., 2021; Ho et al., 2022; J. W. Lee et al., 2020; Sunderland et al., 2019). In particular, research has identified the liver to be a target organ for perfluorooctanesulfonic acid

Received: September 12, 2025. **Revised:** April 28, 2026. **Accepted:** May 5, 2026

(PFOS) accumulation causing hepatoxicity via liver steatosis (Beale et al., 2022; Chang et al., 2014; Costello et al., 2022; Ducatman & Fenton, 2022; J. W. Lee et al., 2020; P. Wang et al., 2022).

Gene expression studies conducted in zebrafish and other vertebrates have shown that PFOS alters transcriptional activity in the livers where lipid metabolism is one of the key pathways commonly affected (Ankley et al., 2021; Beale et al., 2022; J. Chen et al., 2014; Christou et al., 2020; Davidsen et al., 2022; G. Dong et al., 2021; Haimbaugh et al., 2022; Jacobsen et al., 2018; H. Lee et al., 2021; Martínez et al., 2019; Mylroie et al., 2021; Rodríguez-Jorquera et al., 2019; Q. Wang et al., 2022). Specifically, exposure to PFAS such as PFOS, perfluorooctanoic acid, perfluorohexanesulfonic acid, 6:2-fluorotelomersulfonic acid, among others, has been demonstrated to affect transcriptional expression within the peroxisome proliferator–activated receptor (PPAR) pathway, which is key for maintaining lipid homeostasis in the liver in multiple vertebrate species (Beale et al., 2022; J. Chen et al., 2014; Christou et al., 2020; Davidsen et al., 2022; G. Dong et al., 2021; Gust et al., 2019; Haimbaugh et al., 2022; Jacobsen et al., 2018; H. Lee et al., 2021; Martínez et al., 2019; Mylroie et al., 2021; Rodríguez-Jorquera et al., 2019; P. Wang et al., 2022; Q. Wang et al., 2022). In a comprehensive review of omics studies investigating PFAS effects on mammals, fish, reptiles, and amphibians, Beale et al. (2022) identified conserved impacts on PPARα and PPARγ nuclear receptor pathways and associated effects on lipid metabolism–related genes, proteins, and metabolites. Focusing on zebrafish, PFOS and other PFAS exposures have been shown to cause perturbations of transcriptional expression in PPARγ and PPARβ/δ genes in addition to various PPAR-associated transcription factors and cofactors (Mylroie et al., 2021; Rodríguez-Jorquera et al., 2019; Q. Wang et al., 2022). Correspondingly, the PFAS exposures affected transcriptional expression within the overall PPAR nuclear signaling gene network, altering downstream expression of genes involved in lipid metabolism (Haimbaugh et al., 2022; Martínez et al., 2019; Mylroie et al., 2021; Q. Wang et al., 2022) and lipid transport (Christou et al., 2020; Mylroie et al., 2021). Consequences of these responses to PFAS exposures in zebrafish include increased incidences of hepatocellular vacuolation (Q. Wang et al., 2022).

Given the key role of the PPAR isoforms (PPARα, PPARγ, PPARβ/δ) in lipid homeostasis in the liver, perturbations in receptor activation/repression, gene transcription, and/or the signaling cascade can disrupt proper lipid homeostasis in the liver, resulting in adverse outcomes (AOs) including hepatic steatosis (Y. Wang et al., 2020). Hepatic steatosis is part of the progression of nonalcoholic fatty liver disease (NAFLD), which can result in inflammation and liver injury and ultimately nonalcoholic steatohepatitis (Kudaravalli & John, 2023).

As part of a multigenerational exposure investigating the bioaccumulation and effects of PFOS on zebrafish survival, growth, and reproduction (Gust et al., 2024, 2025), liver tissues were collected from zebrafish from the parental (P) and first filial (F1) generations and used in the present study to evaluate hepatoxicity via histopathology and RNA sequencing analysis of male zebrafish liver tissues. In the multigenerational study, males bioaccumulated significantly more PFOS than females in the P and F1 generations (Gust et al., 2025) and were more sensitive to PFOS-induced impacts on growth (Gust et al., 2024). In addition, gross observations of livers from adult P and F1 male fish in the highest concentration showed notable discoloration and possible indication of fatty livers, which were not observed in female or control livers. Therefore, the present histopathology and global transcriptomic expression investigation focused on male livers from the P and F1 generations. The results were integrated with other relevant results from the published literature to generate a draft AO pathway (AOP) linking the molecular initiating event (MIE) of chemical binding (e.g., PFOS) to PPAR, which elicited sequential key events (KEs) of disrupted PPAR nuclear signaling, impaired transcriptional expression for genes involved in lipid metabolism, lipid accumulation in liver, and the AO of liver steatosis.

Methods

Exposure design

Detailed methods for the multigenerational zebrafish exposure are available in the study of Gust et al. (2024). A brief description of the exposure design and methodology is provided here. Zebrafish were exposed continuously to five nominal concentrations of PFOS (0.1, 0.6, 3.2, 20, 100 µg/L) or control (0 µg/L) with five replicates per treatment across three consecutive generations (P, F1, F2). The PFOS concentrations at the low end of the exposure range approach environmentally relevant concentrations while the high end targets potentially affective concentrations in zebrafish. Heptadecafluorooctanesulfonic acid potassium salt from Sigma-Aldrich (CAS No. 2795-39-3, >98% purity, Product No. 77282, Lot No. BCCC4690) was used for all PFOS exposures, and all exposure solutions were prepared in Purofine® PFA694 (Purolite LLC) filtered reverse osmosis water. For the P generation, zebrafish embryos were generated from wild type AB strain adult zebrafish (Zebrafish International Resource Center), which were bred in a single mass spawning event in an iSpawn (Tecniplast) breeding chamber with a ∼2:1 male:female ratio. Embryos were collected and washed (Z. M. Varga & Murray, 2016), and the exposures started at ∼7 hr postfertilization and lasted 180 days. Zebrafish were exposed under static conditions from Day 0 to 5, under static renewal conditions from Day 6 to 30 (80% water exchange twice daily), and under flow-through conditions with a three-times daily volume exchange rate from Day 30 to 180 (2.8 L of exposure solution per replicate tank). Approximately 50 zebrafish embryos were exposed through 111 days postfertilization (dpf); after which, the number of individuals was reduced in each treatment replicate to 30 fish, 15 males and 15 females where possible, to achieve even sex ratios in each replicate for breeding trials. Zebrafish were fed L-type rotifers (Reed Mariculture) and GEMMA Micro 75 (Skretting USA) three times daily for the first 30 days, followed by only GEMMA Micro feed two times daily for the duration of the exposure (GEMMA Micro 75: Days 30–50, Micro 150: Days 50–111, Micro 500: Days 111–180). To generate the F1 generation, all males and females from each replicate in the P generation were bred at 180 dpf in 1.7-L slope breeding tanks (Tecniplast), with breeding events mating only fish within each treatment replicate to ensure the statistical requirement of independence

through the entire exposure. After breeding, the F1 embryos were collected and washed, and approximately 50 fertilized embryos were exposed to the PFOS concentration to which their parents were exposed through 180 dpf following the methods previously described for the P generation.

Tissue collection

At the termination of the P and F1 generations (each at 180 dpf), zebrafish were euthanized by an overdose of buffered 4-g/L tricaine methanesulfonate (MS-222, CAS No. 886-86-2, Product No. A5040; Sigma-Aldrich). After weight and length of the fish were recorded, the livers were removed from a subset of the male fish and either flash-frozen in liquid nitrogen in 1.5-ml tubes for subsequent RNA extraction and transcriptomic analyses or preserved in ∼8-ml Dietrich's fixative (Kent et al., 2012) in 20-ml scintillation vials for subsequent histopathology.

Histotechnology and histopathology

Two liver samples per replicate per treatment ($n = 10$ per treatment) for male liver tissues from the P and F1 generations (control, 20-µg/L, and 100-µg/L treatments) were prepared for histopathological analysis according to standard procedures (Carson & Hladik, 1997). Briefly, tissues were processed to paraffin infiltration by an automated instrument and embedded into paraffin, then the tissue blocks were cut on a rotary microtome. Two glass slides were prepared for each sample, containing a ribbon of three to five sections with a 50-μm step between slides. Tissue thickness was 5 μm. Slides were stained with hematoxylin and eosin and then covered with glass by synthetic mounting media. Low-quality slides were removed from the analysis, resulting in a minimum of eight samples per treatment group for the histopathological evaluation (Table 1).

Liver tissues were assessed for potential treatment- and nonexposure-related lesions based on histopathology best practice guidelines (Crissman et al., 2004). Tissue examinations were not conducted blind; however, evaluation of tissues with knowledge of the treatment conditions is an accepted practice under the guidance used for histopathological analyses in this study (Crissman et al., 2004). Diagnostic criteria and severity scoring methodology were obtained from the U.S. Environmental Protection Agency's Endocrine Disruptor Screening Program and the Organisation for Economic Co-operation and Development's histopathology guidance document (Johnson et al., 2009; Office of Chemical Safety and Pollution Prevention, 2015) and are detailed in the accompanying online supplementary material. Histopathology scores were analyzed for statistical significance against control responses using the Rao–Scott–adjusted Cochran–Armitage test for trends by slices (Green et al., 2014). Differences between control and treatment responses were considered significant at $p \leq 0.05$.

RNA extraction, RNA sequencing, and data analysis

For the transcriptomic analysis, four of the five total replicate exposures for each experimental condition, which included the control and 0.6-, 3.2-, 20-, and 100-µg/L PFOS exposures, were randomly chosen for RNA sequencing analysis for the P and F1 generations. Ultimately, male zebrafish livers from four replicates for each of the five experimental conditions were analyzed for the P and F1 generations. RNA was extracted from liver tissues via the Qiagen RNeasy® Mini Kit per the manufacturer's protocol. Following extraction, RNA quantity was determined by a NanoDrop™ 2000 Spectrophotometer (Thermo Fisher Scientific), and RNA quality was assessed by an Agilent 2200 TapeStation System, with all extractions having an RNA integrity number >8.0.

For sequencing, 100 ng of total RNA was used per sample to prepare libraries with the TruSeq Stranded mRNA Library Preparation Kit with TruSeq RNA Single Indexes, per the manufacturer's instructions (Illumina), where each sample was designated with a unique identifier. The mRNA libraries obtained were assessed with the 4200 TapeStation System (Agilent Technologies), purified with SPRIselect beads (Beckman Coulter), and quantified with the Qubit™ 3.0 Fluorometer. Libraries were normalized and pooled, with 10 per pool. The pools were sequenced over four sequencing runs on a NextSeq 500 System (Illumina) at 1 × 150 cycles, single read, via the NextSeq 500/550 High Output Kit Version 2 following the manufacturer's instructions. Sequencing reads have been submitted to the National Center for Biotechnology Information (NCBI) BioProject database (PRJNA1299447; https://www.ncbi.nlm.nih.gov/bioproject).

Following sequencing, reads were separated for each treatment and checked for quality using FastQC 0.11.9 (Andrews, 2017) and then cleaned in Trimmomatic 0.39 (Bolger et al., 2014) per the following variables: ILLUMINACLIP:TrueSeq3-PE2.fa:2:30:10 SLIDINGWINDOW:4:20 MINLEN:36. Reads were mapped with counts generated for NCBI (GCF_000002035.6) and Ensembl (GRCz11) zebrafish genome assemblies (Harrison et al.,

Table 1 Incidences and severity of selected findings in male liver tissues from the P and F1 generations.

Generation	P			F1		
PFOS, µg/L	**0**	**24**	**101**	**0**	**16**	**75**
Number examined	8	8	9	8	9	10
Hepatocellular vacuolization: Lipid type	4	0	6	0	1	9
Grade 1: Minimal	3		1		1	
Grade 2: Mild	1		4**			4***
Grade 3: Moderate			1			4**
Grade 4: Extensive						1
Hepatocellular vacuolization: Glycogen	8	8	9	8	9	10
Grade 1: None to minimal	4	5	5		1	4*
Grade 2: Moderate	4	3	4	4	5	5
Grade 3: Extensive				4	3	1

Note. Histopathology scores were analyzed for statistical significance against control responses using the Rao–Scott–adjusted Cochran–Armitage test for trends by slices (Green et al., 2014), and differences from control values were considered significant as indicated. Severity grading is detailed in the online supplementary materials. P = parental; F1 = first filial generation; PFOS = perfluorooctanesulfonic acid.

* $p < 0.05$.

** $p < 0.01$.

*** $p < 0.001$.

2024; Pruitt et al., 2014) via STAR 2.7.10b (Dobin et al., 2013). Both assemblies were indexed for STAR to process by STAR's –runmode genomeGenerate with sjdbOverhang set to 35. Genes were filtered by the following conditions: total abundance ≥50, percent coeffecient of variation >0.5, and 50% of samples with an abundance >5. Once all preprocessing was complete, DESeq2 (Love et al., 2014) was used to test for differential expression (DE) and $\log_2$ fold change within and across treatments when compared with the control according to two methodologies: the Wald test and likelihood ratio test (LRT). The Wald tests were used for generation × treatment comparisons to the appropriate control (e.g., 100-µg/L F1 vs. F1 control), and the LRT was used for generation across treatment to appropriate control (e.g., all F1 PFOS vs. F1 control) and for both generations to controls. The raw p value calculated by these methodologies was then adjusted by the Benjamini–Hochberg multiple-test correction method, which controls the false discovery rate to calculate an adjusted p value. A transcript was considered to have significant DE with an adjusted $p < 0.05$ relative to the control. For a more conservative analysis, the transcripts with significant DE in both assemblies (NCBI and Ensembl) were compared for the Wald test, and a list of common DE transcripts from both assemblies was generated for each generation × treatment comparison and across the generations. Furthermore, LRT does not give a reliable measure of transcript fold change direction, only significance and magnitude of change; as such, a list of DE transcripts found in common between the LRT analysis and the complete list of unique DE transcripts by Wald test for each assembly was generated to determine transcripts found in common between the two analysis procedures and provide accurate fold change direction for those transcripts. For all generation × treatment comparisons, the gene counts were based on the transcripts with DE in the NCBI and Ensembl databases.

The DE tables were used with the DAVID bioinformatics system (D. W. Huang et al., 2009; Sherman et al., 2022) to perform pathway enrichment analysis via the Wald- and LRT-generated gene databases and conducted with 3 pathway databases: Kyoto Encyclopedia of Genes and Genomes (KEGG), WikiPathways, and Reactome (Agrawal et al., 2024; Kanehisa, 2019; Kanehisa et al., 2023; Kanehisa & Goto, 2000; Milacic et al., 2024). The cutoff for significant enrichment was a p value <0.05 with a ±2≥ fold enrichment score for pathway enrichment analysis generated from the Wald and LRT test gene expression databases. Additionally, significant DE transcripts (adjusted $p < 0.05$ with ±1 $\log_2$ > fold change) based on Wald and LRT analysis were mapped to homologous human genes using Ensembl (Harrison et al., 2024), and pathway enrichment analysis was conducted in Qiagen Ingenuity Pathway Analysis (IPA®) software (https://digitalinsights.qiagen.com/IPA; Krämer et al., 2014). Pathways were considered significant if they had a p value <0.05, and a z score was calculated (IPA; Krämer et al., 2014) for each significant pathway to calculate the likelihood that the pathway was activated (z score ≥2) or inhibited (z score ≤−2) or that no conclusion could be drawn (z score = 0).

AOP development

A draft AOP was developed using the guidelines in the AOP *Developer's Handbook 2.6* (Villeneuve et al., 2023) incorporating empirical evidence derived from the present study and other studies from our laboratory (Albers et al., 2024; Mylroie et al., 2021), as well as a comprehensive literature review of peer-reviewed publications related to PPAR, PFAS, liver steatosis, and lipid metabolism identified through Web of Science™ and Google Scholar searches. In vivo, in vitro, and in silico studies involving aquatic and terrestrial vertebrates were used as evidence for the development of the AOP. Dose–response relationships were not quantitatively established during the development of this AOP.

Results

The measured cumulative PFOS concentrations from the 180-day exposures were 0.72, 3.4, 24, and 101 µg/L in the P generation and 0.48, 2.5, 16, and 75 µg/L in the F1 generation, where details on sample size and variance are presented in online supplementary material Table S1. For the purposes of the *Results* and *Discussion* sections, we prioritized using the measured PFOS concentrations when describing effects for a treatment in an individual generation, but we use nominal concentrations when generalizing PFOS exposures across generations where measured concentrations differ slightly for the same PFOS treatment. In the *Results* and *Discussion* sections, use of measured concentrations is indicated by "mea." for measured after the PFOS treatment value, and use of nominal concentrations is indicated by "nom." for nominal after the PFOS treatment value.

Histopathology

An increase in the number and severity of lipid-type hepatocellular vacuolation was observed in the P generation males exposed to PFOS (6/9 samples) at 101 µg/L (mea.) as compared with the control males (4/8 samples), with significant effects ($p < 0.01$) at the mild grade (4/9 samples) versus the control (1/8 samples; Table 1). More prevalent and pronounced histopathological effects were observed in the F1 generation males exposed to PFOS at 75 µg/L (mea.), where lipid-type vacuolation (9/10 samples) was significant at mild ($p < 0.001$) to moderate ($p < 0.01$) grades (8/10) as compared with the control (0/8; Table 1, Figure 1, online supplementary material Figure S1). Furthermore, an associated significant co-occurrence ($p < 0.05$) of decreased hepatocellular glycogen vacuolation was observed in the 75-µg/L PFOS (mea.) exposure relative to controls in the F1 generation. There were no significant observations of lipid-style hepatocellular vacuolation relative to the controls in the 20-µg/L PFOS (nom.) treatment from either the *P* (24 µg/L mea.) or F1 (16 µg/L mea.) generation.

Transcriptomic expression analysis

Two-dimensional principal component analysis (PCA) showed that the two principal components accounted for only ∼50% of the variation. A minor degree of cluster separation was driven by the generation, while the PFOS exposure treatment showed no cluster separation except in the 100-µg/L (nom.) treatment, which displayed partial cluster separation (online supplementary material Figure S2). The PFOS exposures caused an increased number of differentially expressed transcripts (DETs) in

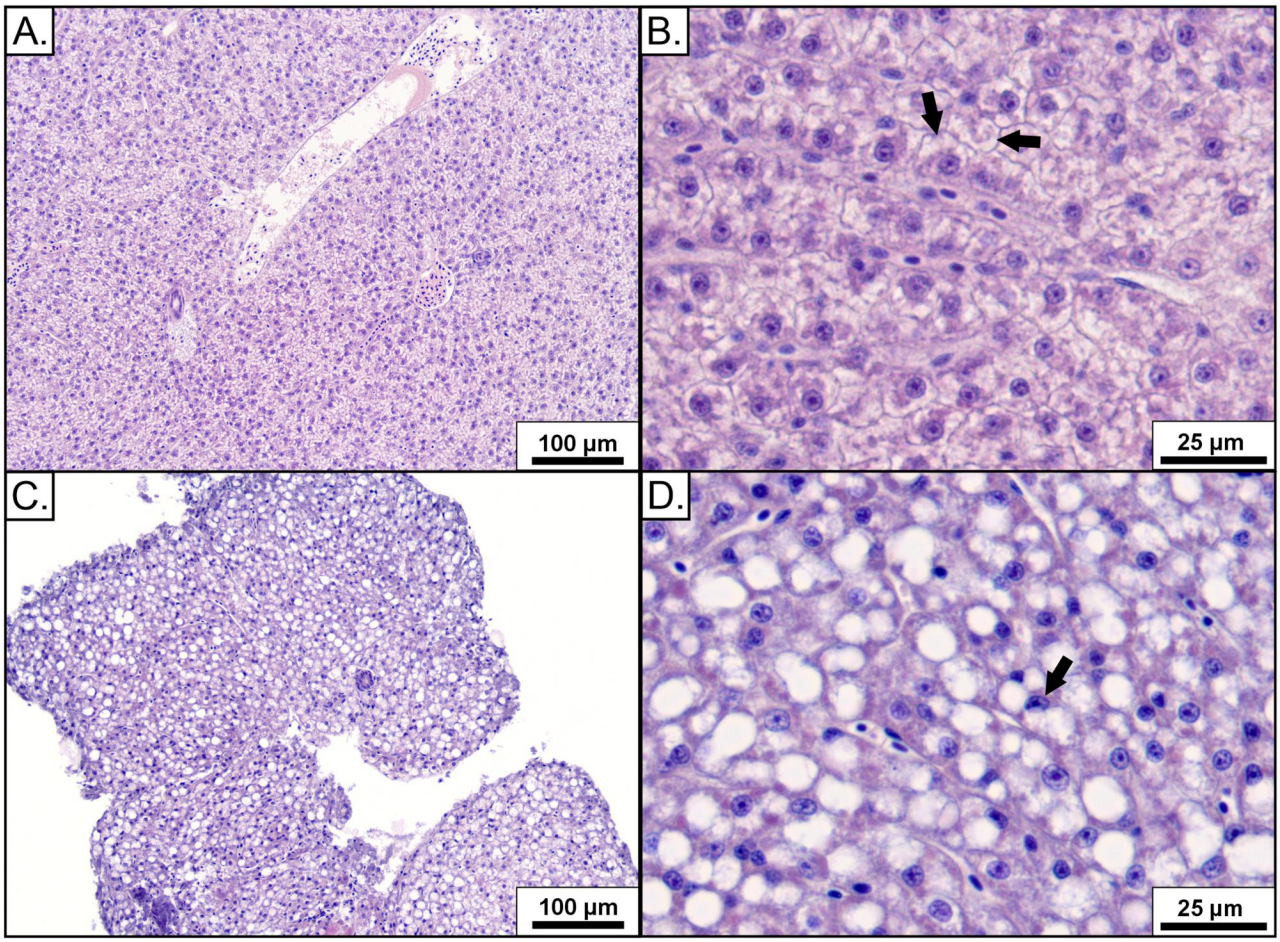

Figure 1. Liver histopathology in male zebrafish from the first filial (F1) generation. (A) Control zebrafish liver tissues from the F1 generation. (B) Higher magnification of panel A. No lipid vacuolation was observed, but regions of glycogen vacuolation can be visualized within hepatocytes (arrows). Glycogen vacuolation appears angular and irregularly shaped, with lightly stained flocculent contents. (C) Liver from an F1 generation male, 75 µg/L (measured). Grade 4 hepatocellular vacuolation, lipid type. (D) Higher magnification of panel C. The intracellular lipid vacuoles appear round and clear and can distort the cell and compress nuclei (arrow). In hepatocytes containing lipid vacuoles, the glycogen vacuolation was greatly reduced. Hematoxylin and eosin stain. Bar: 100 µm (A, C); 25 µm (B, D).

the F1 generation versus the P generation across all unique DET accessions identified by the Wald test (adjusted $p < 0.05$, ±1 $\log_2 \geq$ fold change) for all accessions matching in the Ensembl and NCBI databases (Table 2). When comparing all unique DETs from each treatment having common accessions in the Ensembl and NCBI databases from the Wald test and LRT analysis (adjusted $p < 0.05$, ±1 $\log_2 \geq$ fold change), we were able to identify DETs found in common between zebrafish generations, which are provided in Figure 2 and Figure 3. The Ensembl and NCBI identities from DETs revealed in the LRT analysis and the Wald test were compared, and a list of DETs (adjusted $p < 0.05$, ±1 $\log_2 \geq$ fold change) found in common was generated for each generation (online supplementary material Table S2). Comparison of DET identities between Ensembl and NCBI annotations identified greater commonality within generations versus that between the P and F1 generations, where only eight DETs were found in common (Figure 2 and Figure 3). For the common genes, the directional expression, based on Wald test values, matched for six of the eight transcripts (Figure 3). In the combined DET list (significant DE, adjusted $p < 0.05$, ±1 $\log_2 \geq$ -fold change, in LRT and Wald test in both assembly databases), a significant DE of 68 transcripts (34 increased and 34 decreased) was observed relative to controls for the P generation, while 417 had significant DE (18 increased and 399 decreased) relative to controls in the F1 generation. Finally, when the P and F1 generations were combined and examined for effects of PFOS exposure by LRT analysis only, 320 transcripts had significant DE (adjusted $p < 0.05$, ±1 $\log_2 \geq$ fold change) relative to controls.

When comparisons were performed for generation × treatment with the respective controls, Wald tests (adjusted $p < 0.05$, ±1 $\log_2 \geq$ fold change) identified that livers from fish exposed to PFOS at 75 µg/L (mea.) from the F1 generation had the highest number of significant DETs (946) relative to controls (for a summary of all generation × treatment comparisons, see Table 2). For the P generation, the 0.72-µg/L (mea.) treatment had the greatest number of DETs, with a total of 64 transcripts being differentially expressed. Interestingly, the livers from fish exposed

Table 2 Differentially expressed transcripts (DETs) in P and F1 generations by treatment combination versus controls for genes in common between National Center for Biotechnology Information and Ensembl assemblies, including the number of unique DETs overall for each generation.

Generation: PFOS treatment, μg/L [a]	Genes		
	Total	Increased	Decreased
P			
0.72	64	25	39
3.4	7	4	3
24	22	11	11
101	24	18	6
All [b]	103	50	53
F1			
0.48	8	3	5
2.5	6	2	4
16	8	5	3
75	946	182	764
All [b]	955	188	767

Note. Comparisons are based on (adjusted $p < 0.05$, $\pm 1 \log_2 >$ fold change) the Wald test. P = parental; F1 = first filial generation; PFOS = perfluorooctanesulfonic acid.

[a]Mean cumulative measured PFOS concentrations (Gust et al., 2024).

[b]*All* refers to all unique DETs for entire generations. Each generation × treatment comparison was compared with all others for a given generation, and all DETs for that generation were compiled into one list with duplicates counted only once.

to PFOS at 101 μg/L (mea.) in the P generation had only 24 DETs as compared with controls. Complete Wald test results for significant DE transcripts are available in online supplementary material Tables S3 and S4, and full DE analysis statistics for all genes across all comparisons for Wald test and LRT analysis are presented in online supplementary material Tables S5 and S6.

Pathway enrichment analysis

The DAVID-based pathway enrichment analysis of significant DETs resulting from all PFOS exposures relative to controls for the combined P and F1 generations identified significant enrichment ($p \leq 0.05$, fold enrichment ≥ 2) of 8 KEGG, 27 Reactome, and 2 WikiPathway pathways (online supplementary material Table S7). When enrichment was investigated separately for each generation, PFOS exposure in the F1 generation resulted in significant enrichment ($p \leq 0.05$, fold enrichment ≥ 2) of 5 KEGG, 54 Reactome, and 2 WikiPathway pathways as compared with the control, while only 1 KEGG, 1 Reactome, and 0 WikiPathway pathways were enriched ($p \leq 0.05$, fold enrichment ≥ 2) in response to PFOS in the P generation as compared with the control. Investigation of pathway enrichment by PFOS dose as compared with the control identified few significantly enriched pathways ($p \leq 0.05$, fold enrichment ≥ 2) in PFOS exposure doses < 100 μg/L (nom.) and primarily within the F1 generation. The five most enriched pathways for each treatment comparison (where applicable) are summarized in Table 3. For the complete list of significantly enriched pathways ($p \leq 0.05$, fold enrichment ≥ 2), see online supplementary material Table S7.

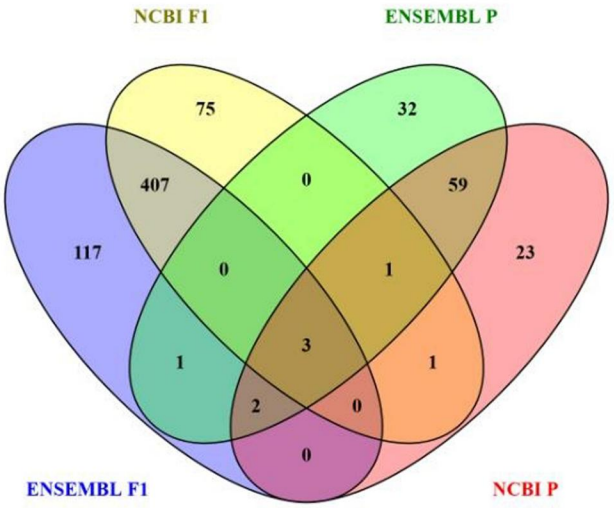

Figure 2. Venn diagram showing the number of differentially expressed transcripts in the parental (P) and first filial (F1) generations across all treatment concentrations by each mapped assembly (National Center for Biotechnology Information [NCBI] and Ensembl; adjusted $p < 0.05$, $\pm 1 \log_2 \geq$ fold change). Area where the circles overlap shows the number of gene IDs that were differentially expressed in common between the two generations and/or between the two mapping assemblies. Created with Venny Tool (Oliveros, 2007).

The IPA-based pathway enrichment analysis using human homologs to zebrafish DETs identified 114 unique, significantly enriched canonical pathways ($p \leq 0.05$) in the PFOS-exposed zebrafish across both generations and treatments as compared with controls (online supplementary material Table S8). Similar to the DAVID pathway analyses, the F1 generation had a greater number of significantly enriched pathways ($p \leq 0.05$) relative to the P generation with the majority in response to the highest PFOS exposure (100 μg/L nom.). The five most enriched pathways for each treatment comparison (where applicable) are summarized in Table 4. For the complete list of significantly enriched pathways, see online supplementary material Table S8. Finally, as part of the IPA, the top toxicity pathways were identified from comparisons across each generation and within each generation by treatment. There was significant overrepresentation of toxicity pathways across and within each generation at $p \leq 0.05$ (Table 5) with multiple ones associated with liver toxicity or lipid metabolism. The top five toxicity results for the across-generation comparisons and the 100-μg/L (nom.) generation × treatment comparisons (where applicable) are presented in Table 5, and full results for all generation × treatment comparisons are available in online supplementary material Table S9.

Draft AOP

Using results from the present study with observations from peer-reviewed literature, we developed the AOP titled "Xenobiotic binding to peroxisome proliferator–activated receptors (PPARs) causes dysregulation of lipid metabolism leading to liver steatosis," which was submitted to AOP-Wiki (Society for

Ensembl ID	Gene ID	Gene Name	Transcript Expression	
			P	F1
			Log_2FC (± SE)	
ENSDARG00000092233	vtg1	vitellogenin 1	-9.16 (± 1.60)	-8.46 (± 1.77)
ENSDARG00000055809	vtg2	vitellogenin 2	-9.39 (± 1.67)	-9.26 (± 2.00)
ENSDARG00000016448	vtg3	vitellogenin 3	-8.67 (± 1.60)	-8.04 (± 1.71)
ENSDARG00000099824	nots	nothespin	-7.58 (± 1.36)	-5.36 (± 1.38)
ENSDARG00000089461	ciz1b	cdkn1a interacting zinc finger protein 1b	-1.49 (± 0.38)	-2.56 (± 0.66)
ENSDARG00000061885	satb2	SATB homeobox 2	-4.77 (± 1.22)	3.13 (± 0.76)
ENSDARG00000035438	myhc4	myosin heavy chain 4	-5.39 (± 1.48)	5.31 (± 1.81)
ENSDARG00000015862	rpl5b	ribosomal protein L5b	9.13 (± 1.82)	7.71 (± 1.89)

Figure 3. Common differentially expressed transcripts (adjusted $p < 0.05$, ±1 $\log_2 \geq$ fold change [Log_2FC]) between parental and first filial generations for all perfluorooctanesulfonic acid treatments as compared with controls in the Wald test and likelihood ratio test analysis for all common accessions found between the Ensembl and National Center for Biotechnology Information assemblies. Red, increased expression; green, decreased expression. Log_2FC based on values derived from Wald test analyses. P = parental; F1 = first filial generation.

Advancement of AOPs, 2023; AOP 529). The AOP represents the plausible concept for mechanistic toxicity of a chemical contaminant (here represented by PFOS) binding the PPAR isoforms, which disrupts PPAR signaling and thus lipid metabolism, resulting in lipid accumulation in the liver leading to the AO of liver steatosis (Figure 7).

Discussion

Histopathology

Histopathology for livers collected from male zebrafish exposed to PFOS at 0, 20, and 100 µg/L (nom.) through 180 dpf in the P and F1 generations identified significantly increased incidences and severity of lipid-style hepatocellular vacuolation in the 100-µg/L (nom.) exposure relative to controls (Table 1). Evidence of lipid accumulation in male livers was also observed in previous studies investigating PFOS exposure in zebrafish (Cheng et al., 2016; Y. Cui et al., 2017; Du et al., 2009; J. Huang, Liu, et al., 2022; Keiter et al., 2012; Q. Wang et al., 2022). Furthermore, hepatic lipid accumulation has been reported in rats, mice, and frogs exposed to PFOS (L. Cui et al., 2009; Davidsen et al., 2022; Huck et al., 2018; Lin et al., 2022; Rosen et al., 2010; Salter et al., 2021; L. Zhang et al., 2016). In the present study, livers from the F1 generation male zebrafish exposed to the highest PFOS exposure concentration (75 µg/L mea.) exhibited a greater number and severity of lipid-style hepatocellular vacuolation incidences, which suggests the potential growing severity of hepatic impacts in continuous PFOS exposures throughout two generations. Moreover, the livers of the F1 generation male zebrafish exposed to PFOS at 75 µg/L (mea.) displayed decreased glycogen vacuolation as compared with the controls, suggesting potentially decreased incorporation of readily available cellular energy substrates into glycogen, which may have contributed to observations of reduced body weights in response to the 100-µg/L (nom.) PFOS exposures (Gust et al., 2024). An increase in lipid accumulation in livers with a simultaneous decrease in glycogen following PFOS exposure has been observed in other vertebrate species including mice (L. Wang et al., 2014). Overall, these results confirm previous findings linking PFOS exposure to lipid accumulation in livers and suggest that continuous exposure across generations may result in increased severity of lipid accumulation in the liver.

Transcriptomics and pathway analyses

Transcriptomic analysis of liver tissue collected from zebrafish exposed to PFOS through 180 dpf across two generations exhibited significant DETs and significant enrichment of multiple functional pathways, primarily in response to the highest PFOS exposure concentration (100 µg/L nom.), increasing from the P generation to the F1 (Table 2, Figure 2). The correspondence of more pronounced effects of PFOS for the histopathological responses and transcriptional effects in zebrafish liver tissue in the F1 generation versus the P generation suggests the potential for compounding effects of continuous PFOS exposure across generations. For the P generation, it should be noted that the lowest exposure concentration (0.72 µg/L mea.) had the greatest number of DETs, and all treatment concentrations in the P generation had relatively low numbers of DETs (<100) as compared with the controls. Aside from the greatly increased number of significantly affected transcripts at the 75-µg/L (mea.) PFOS exposure in the F1 generation, no clear dose–response relationships were observed between the lower PFOS exposure concentrations and the number of significantly affected transcripts.

Table 3 Significantly enriched pathway terms following Kyoto Encyclopedia of Genes and Genomes (KEGG), Reactome, and WikiPathways pathway analysis.

Comparison: Term	*p* value	Fold enrichment
KEGG		
P + F1: All PFOS concentrations		
dre00100: Steroid biosynthesis	2.4E-04	15.74
dre04110: Cell cycle	1.5E-03	3.65
dre04914: Progesterone-mediated oocyte maturation	5.2E-03	4.33
dre04114: Oocyte meiosis	5.7E-03	3.67
dre04814: Motor proteins	2.9E-02	2.45
F1: All PFOS concentrations		
dre00100: Steroid biosynthesis	3.4E-08	16.05
dre04110: Cell cycle	5.7E-08	4.81
dre04914: Progesterone-mediated oocyte maturation	7.4E-07	5.25
dre04114: Oocyte meiosis	1.1E-04	3.64
dre00900: Terpenoid backbone biosynthesis	2.0E-03	8.92
P: All PFOS concentrations		
dre04068: FoxO signaling pathway	1.5E-02	3.06
F1: 100-μg/L PFOS		
dre04110: Cell cycle	1.0E-13	5.61
dre04914: Progesterone-mediated oocyte maturation	2.2E-08	5.08
dre04114: Oocyte meiosis	2.2E-06	3.77
dre04120: Ubiquitin mediated proteolysis	8.8E-04	2.79
dre04218: Cellular senescence	1.5E-02	2.10
P: 0.6-μg/L PFOS	2.9E-02	10.61
dre04137: Mitophagy–animal		
Reactome		
P + F1: All PFOS concentrations		
R-DRE-69620: Cell cycle checkpoints	2.04E-04	3.86
R-DRE-141424: Amplification of signal from the kinetochores	5.82E-04	6.56
R-DRE-141444: Amplification of signal from unattached kinetochores via a MAD2 inhibitory signal	5.82E-04	6.56
R-DRE-5617833: Cilium assembly	9.57E-04	4.97
R-DRE-9648025: EML4 and NUDC in mitotic spindle formation	1.31E-03	5.63
F1: All PFOS concentrations		
R-DRE-5617833: Cilium assembly	4.70E-13	6.96
R-DRE-1852241: Organelle biogenesis and maintenance	2.22E-11	5.81
R-DRE-1640170: Cell cycle	1.06E-10	2.98
R-DRE-69278: Cell cycle, mitotic	9.47E-10	3.07
R-DRE-68877: Mitotic prometaphase	7.71E-08	4.64
P: all PFOS concentrations		
R-DRE-1266738: Developmental biology	0.02177	2.80
F1: 100-μg/L PFOS		
R-DRE-1640170: Cell cycle	8.40E-21	3.47
R-DRE-69278: Cell cycle, mitotic	9.70E-19	3.57
R-DRE-5617833: Cilium assembly	1.10E-14	6.17
R-DRE-1852241: Organelle biogenesis and maintenance	1.31E-12	5.15
R-DRE-68886: M phase	2.56E-12	3.33
P: 100-μg/L PFOS		
R-DRE-597592: Posttranslational protein modification	0.028811	3.39
WikiPathways		
P + F1: All PFOS concentrations		
WP1387: Cholesterol biosynthesis	1.77E-06	24.50
WP1393: Cell cycle	2.63E-04	5.63
F1: All PFOS concentrations		
WP1387: Cholesterol biosynthesis	8.82E-13	23.29
WP1393: Cell cycle	9.62E-07	5.11
F1: 100-μg/L PFOS		
WP1393: Cell cycle	6.83E-12	6.68
WP451: DNA replication	0.001371	5.35

Note. Top 5 terms shown for each. Cutoff for significant enrichment was $p \leq 0.05$, fold enrichment ≥ 2. PFOS treatment values for individual generation × treatment comparisons represent the nominal PFOS concentration values. P = parental; F1 = first filial generation; PFOS = perfluorooctanesulfonic acid.

Table 4 Ingenuity Pathway Analysis canonical pathway analysis results.

Comparison: Ingenuity canonical pathway	*p* value	*z* score
P + F1: All PFOS concentrations		
Kinetochore metaphase signaling pathway	2.00E-07	1.897
Cholesterol biosynthesis I	4.79E-07	−2.236
Cholesterol biosynthesis II (via 24,25-dihydrolanosterol)	4.79E-07	−2.236
Cholesterol biosynthesis III (via desmosterol)	4.79E-07	−2.236
Superpathway of cholesterol biosynthesis	1.58E-06	−2.449
F1: All PFOS concentrations		
Kinetochore metaphase signaling pathway	2.51E-11	2.183
Mitotic roles of polo-like kinase	6.46E-09	1.897
Noradrenaline and adrenaline degradation	5.89E-07	2.828
Ethanol degradation II	4.90E-06	2.646
Serotonin degradation	5.89E-04	2.646
P: All PFOS concentrations		
Pyrimidine ribonucleotides interconversion	1.62E-03	—
Pyrimidine ribonucleotides de novo biosynthesis	2.04E-03	—
Pyrimidine deoxyribonucleotides de novo biosynthesis I	9.12E-03	—
Spermine biosynthesis	1.26E-02	—
Spermidine biosynthesis I	1.26E-02	—
F1: 100-μg/L PFOS		
Kinetochore metaphase signaling pathway	3.16E-17	−2.746
Mitotic roles of polo-like kinase	1.48E-09	−2.496
Dermatan sulfate biosynthesis (late stages)	2.88E-06	1.897
DNA damage-induced 14-3-3σ signaling	7.08E-06	0
Dermatan sulfate biosynthesis	3.72E-05	1.897
P: 100-μg/L PFOS		
Iron homeostasis signaling pathway	6.92E-03	—
Bile acid biosynthesis, neutral pathway	1.23E-02	—
Hepatic cholestasis	1.32E-02	—
DNA double-strand break repair by non-homologous end joining	1.32E-02	—
Granzyme B signaling	1.51E-02	—

Note. Table shows the five most enriched pathways for each treatment comparison (where applicable). Pathways were considered significant if $p < 0.05$, and the *z* score represents the likelihood that the pathway was activated (*z* score ≥2) or inhibited (*z* score ≤−2), no conclusion could be drawn (*z* score = 0), or there was no definable pattern (—). PFOS treatment values for individual generation × treatment comparisons represent the nominal PFOS concentration values. PFOS = perfluorooctanesulfonic acid; P = parental; F1 = first filial generation.

Transcriptional expression of vitellogenin-related genes

Comparison of gene transcripts significantly altered by the PFOS exposure revealed few transcripts affected in common between the P and F1 generations, although expression for these genes was largely similar between the generations (Figure 3). One gene family affected similarly among generations was vitellogenin (*vtg*), where transcriptional expression for three gene identities (*vtg1*, *vtg2*, *vtg3*) was decreased in the P and F1 generations. Vitellogenins are mainly produced in the liver of male and female zebrafish with much greater innate production occurring in female fish, where vitellogenins are precursors for essential nutritional components of egg yolks in fish and all other oviparous and ovoviviparous species (Yilmaz et al., 2019). Estrogen or estrogenic compound exposure can induce increased vitellogenin production in male fish; thus, it has become a popular biomarker for determining if exposure to a contaminant has potential estrogenic effects (Denslow et al., 1999). The decreased expression of three vitellogenin transcripts in the livers of male zebrafish exposed to PFOS suggests repression of what is already baseline vitellogenin production in the male fish due to PFOS exposure. These results agree with observations in whole-body vitellogenin analysis conducted in male fish from the P and F1 generations of this exposure, as reported by Gust et al. (2024), which showed no significant vitellogenin production in any treatment or generation. In contrast to these results, Du et al. (2009) noted increased vitellogenin transcript expression in the livers of juvenile and adult zebrafish exposed to PFOS, and Keiter et al. (2012) observed significant production of vitellogenin in the first and second generations of zebrafish males chronically exposed PFOS, although results from each study were nonmonotonic with PFOS dose and sporadic through the exposure duration. Keiter et al. (2012) hypothesized that a lack of significant vitellogenin production in males observed after exposure to higher concentrations of PFOS (300 µg/L) could be due to a decrease in liver fitness attributed to PFOS exposure, which could ultimately inhibit vitellogenin production by the liver itself; in a similar finding, Du et al. (2009) saw no significant difference in vitellogenin transcript expression in zebrafish after 70 days of exposure to 250-µg/L PFOS. Therefore, the decrease in vitellogenin transcript expression seen in the present study may be a result of reduced liver fitness resulting from continuous PFOS exposure, as evidenced by significantly increased incidences of lipid-style hepatocellular vacuolation in P and F1 generations exposed to the highest PFOS concentration (101 and 75 µg/L mea., respectively). However, the reduced transcriptional expression of vitellogenin could also be due to its role in other nonreproductive biological functions, such as innate immune response and response to oxidative stress (C. Sun & Zhang, 2015). Ultimately, more focused investigations would be needed to determine the relationship among PFOS exposure, decreased baseline vitellogenin in males, and any adverse biological responses.

Enrichment of PPAR nuclear signaling pathways

Perfluorooctanesulfonic acid exposures caused significant enrichment of the PPAR pathway (Table 3, Figure 4), the associated nuclear receptors retinoid X receptor/pregnane X receptor (RXR/PXR), and the coordinated lysosomal expression and regulation (CLEAR) signaling pathway (Table 4, Figure 4). Peroxisome proliferator–activated receptors are a family of nuclear receptors in vertebrates that bind lipids as signaling molecules, resulting in a cascade of transcriptional regulatory events that maintain

Table 5 Ingenuity Pathway Analysis top toxicity list results.

Comparison: Ingenuity toxicity lists	*p* value
P + F1: All PFOS concentrations	
Cholesterol biosynthesis	3.89E-08
Cytochrome P450 panel—substrate is a xenobiotic (human)	8.32E-05
Cytochrome P450 panel—substrate is a xenobiotic (rat)	6.17E-04
PXR/RXR activation	1.66E-03
Increases liver hyperplasia/hyperproliferation	1.95E-03
F1: All PFOS concentrations	
Fatty acid metabolism	8.91E-04
Cytochrome P450 panel—substrate is a xenobiotic (human)	9.55E-04
Cytochrome P450 panel—substrate is a xenobiotic (rat)	3.89E-03
Increases liver hyperplasia/hyperproliferation	3.89E-03
Cell cycle: G2/M DNA damage checkpoint regulation	9.33E-03
P: All PFOS concentrations	
Cardiac fibrosis	4.68E-03
CAR/RXR activation	1.45E-02
Fatty acid metabolism	2.40E-02
Genes upregulated in response to chronic renal failure (rat)	2.51E-02
Cytochrome P450 panel—substrate is a vitamin (human)	3.72E-02
F1: 100-μg/L PFOS	
Cell cycle: G2/M DNA damage checkpoint regulation	1.15E-04
LPS/IL-1 mediated inhibition of RXR function	5.50E-03
Cell cycle: G1/S checkpoint regulation	1.35E-02
Positive acute phase response proteins	2.57E-02
Genes downregulated in response to chronic renal failure (rat)	2.69E-02
P: 100-μg/L PFOS	
Genes upregulated in response to chronic renal failure (rat)	3.80E-03
Long-term renal injury pro-oxidative response panel (rat)	1.23E-02
Hepatic cholestasis	1.32E-02
Cytochrome P450 panel—substrate is a sterol (human)	1.32E-02
Cytochrome P450 panel—substrate is a sterol (mouse)	1.32E-02

Note. Table shows the five most enriched pathways for each treatment comparison (where applicable). Pathways were considered significant if $p < 0.05$. PFOS treatment values for individual generation × treatment comparisons represent the nominal PFOS concentration values. P = parental; F1 = first filial generation; PFOS = perfluorooctanesulfonic acid.

energy homeostasis (Grygiel-Górniak, 2014). Specifically, PPARα is integral in regulating fatty acid catabolism and energy production through β-oxidation; PPARγ regulates fatty acid synthesis and storage; and PPARβ/δ plays a key role in glucose homeostasis and β-oxidation (Grygiel-Górniak, 2014; Gust et al., 2019; Lamas Bervejillo & Ferreira, 2019; T. Varga et al., 2011). Despite their more discrete roles, the crosstalk among all PPAR isoforms is essential to maintaining energy homeostasis; therefore, any impacts on the PPAR signaling network can have deleterious outcomes for the organism.

Transcripts having significantly altered expression in the PPAR signaling and associated pathways in the P and F1 generations included apolipoprotein A-Ia (*apoa1a*), fatty acid–binding protein 7a (*fabp7a*), transcription factor EB (*tfeb*), cytochrome P450 family 8 subfamily B member 1 (*cyp8b1*), and PPARγ-related coactivator 1 (*pprc1*), among others. In the F1 generation, *apoa1a* was overexpressed in PFOS-exposed livers when compared with the control, and this phenomenon of overexpression of the *apoa1a* gene has been observed in other studies where zebrafish have been exposed to PFOS (Tse et al., 2016). Increased APOA1A protein can be used as a diagnostic marker for liver fibrosis resulting from chronic liver inflammation in NAFLD and other liver diseases (Gumilas et al., 2022); thus, the overexpression of the *apoa1a* transcript may be a result of the more severe lipid-style hepatocellular vacuolization observed in the livers in F1 males exposed to PFOS causing chronic liver inflammation. In contrast, *fabp7a* expression was significantly decreased in the livers of PFOS-exposed F1 males as compared with the control. A decrease in fatty acid–binding proteins (FABPs) over time as the result of low-dose PFOS exposure has been observed in zebrafish, with Khazaee et al. (2020) noting an initial increase in liver FABPs followed by a significant decrease by Day 30 in zebrafish exposed to 100-µg/L PFOS. The primary function of FABPs is to bind their ligand (fatty acids) and facilitate the transfer to various intracellular compartments for storage or signal transduction initiated by receptors such as PPAR (Xu et al., 2022). However, FABPs may have other roles, such as the regulation of macrophages including Kupffer cells, which are found in the liver (Nguyen-Lefebvre & Horuzsko, 2015). Kupffer cells are involved in the progression of NAFLD where their activation can result in increased liver inflammation, which can result in liver injury. Specifically, investigations in mice have shown that FABP7 may play a role in regulation of

KEGG Pathway dre03320:PPAR signaling pathway

Gene ID	Gene Name		P	F1	LRT P	LRT F1	LRT P+F1
ENSDARG00000104495	Phospholipid transfer protein (pltp)				*		*
ENSDARG00000012076	Apolipoprotein A-Ia (apoa1a)			10.32		*	*
ENSDARG00000007697	Fatty acid binding protein 7 a (fabp7a)			-3.91		*	*
ENSDARG00000093313	Ubiquitin B (ubb)		7.38				*
ENSDARG00000103025	3-hydroxy-3-methylglutaryl-CoA synthase 1 (hmgcs1)					*	*

IPA Canonical Pathways PXR/RXR Activation

Zebrafish Gene ID	Gene Name	Molecule ID	P	F1	LRT P	LRT F1	LRT P+F1
ENSDARG00000070021	cytochrome P450 family 3 subfamily A member 4	CYP3A4					*
ENSDARG00000069018	cytochrome P450 family 7 subfamily A member 1	CYP7A1					*
ENSDARG00000009477	protein kinase cAMP-dependent type II regulatory subunit alpha	PRKAR2A					*
ENSDARG00000103800	protein kinase cAMP-dependent type I regulatory subunit beta	PRKAR1B		-5.36		*	
ENSDARG00000033662	stearoyl-CoA desaturase	SCD				*	

IPA Canonical Pathways Hepatic Cholestasis

Zebrafish Gene ID	Gene Name	Molecule ID	P	F1	LRT P	LRT F1	LRT P+F1
ENSDARG00000097559	cytochrome P450 family 8 subfamily B member 1	CYP8B1	4.92		*		
ENSDARG00000090337	PPARG related coactivator 1	PPRC1	3.73		*		

IPA Canonical Pathways CLEAR Signaling Pathway

Zebrafish Gene ID	Gene Name	Molecule ID	P	F1	LRT P	LRT F1	LRT P+F1
ENSDARG00000011027	fibroblast growth factor receptor 1	FGFR1			*		*
ENSDARG00000002285	mucolipin TRP cation channel 1	MCOLN1	-2.05		*		
ENSDARG00000040072	serine carboxypeptidase 1	SCPEP1			*		
ENSDARG00000010794	transcription factor EB	TFEB	-4.29		*		*
ENSDARG00000067626	tyrosine 3-monooxygenase/tryptophan 5-monooxygenase activation protein gamma	YWHAG			*		

Figure 4. Transcripts and fold change from selected peroxisome proliferator–activated receptor (PPAR)-related pathways. Green cell indicates downregulation and red cell upregulation as compared with the control for at least one generation × treatment comparison based on the Wald test (adjusted $p < 0.05$, $\pm 1 \log_2 \geq$ fold change). Yellow box with an asterisk (*) indicates a transcript that was differentially expressed (adjusted $p < 0.05$) as compared with the control in each likelihood ratio test (LRT) comparison for each generation (P, F1) and across generations (P + F1). Additional tables with fold change information can be found in online supplementary material Table S8. P = parental; F1 = first filial generation; RXR/RXR = retinoid X receptor/pregnane X receptor; CLEAR = coordinated lysosomal expression and regulation; KEGG = Kyoto Encyclopedia of Genes and Genomes; IPA = Ingenuity Pathway Analysis.

Kupffer cell activity in response to damaged hepatocytes (Miyazaki et al., 2014). Therefore, the dysregulation of *fabp7a* observed in the male zebrafish livers after PFOS exposure may be a result of ongoing hepatocyte damage due to PFOS-induced lipid accumulation in the liver.

In the P generation, *tfeb*, which plays a key role in the regulation of lysosome function, autophagy, and lipid metabolism, had significantly decreased expression as compared with the controls in male zebrafish livers (Figure 4). Transcription factor EB (TFEB) plays a role in the regulation of PPARγ-related coactivator 1α and PPAR-α (Yan, 2022). Decreased expression of *tfeb* has been observed in mice suffering from alcohol-induced liver disease with associated liver injury and steatosis, and overexpression of *tfeb* has been shown to improve the prognosis of NAFLD in mice, such as a reduction in lipid accumulation in the liver (Chao et al., 2018; Gong et al., 2022; Yan, 2022). Furthermore, mucolipin transient receptor potential cation channel 1a (*mcoln1a*), which is regulated by TFEB and necessary for lysosome trafficking and storage, had decreased expression. Dysregulation of *mclon1a* has been shown to reduce lipophagy in HepG2 cells; thus, decreased expression of *mcoln1a* may be indicative of a reduction in lipid droplet autophagy, which is important for maintaining lipid homeostasis (S. Zhang et al., 2022).

In the P generation, *pprc1* and *cyp8b1* showed increased expression relative to the control, and expression of both genes has been shown to increase in response to PFOS exposure in previous studies involving zebrafish and mice (Mylroie et al., 2021; R. Zhang et al., 2024). In addition, *pprc1* is part of the PPARγ coactivator 1 family, which is integral for the proper regulation of numerous cellular functions, including fatty acid metabolism and oxidative phosphorylation; along with *cyp8b1* and *cyp7b1*, it helps to regulate bile acid synthesis, which is critical in cholesterol homeostasis and the regulation of lipid metabolism (J. Liu et al., 2022). The overexpression of these genes is further evidence of dysregulation of the PPAR and associated pathways and highlights an overall trend of transcriptional disruption of PPAR-mediated lipid metabolism pathways, which can result in lipid accumulation and associated damage in livers.

WikiPathways WP1387~Cholesterol biosynthesis

Gene ID	Gene Name		P	F1	LRT P	LRT F1	LRT P+F1
ENSDARG00000079946	Squalene epoxidase a (sqlea)					*	*
ENSDARG00000061274	Lanosterol synthase (lss)					*	*
ENSDARG00000099336	Mevalonate (diphospho) decarboxylase a (mvda)					*	
ENSDARG00000055876	Methylsterol monooxygenase 1 (msmo1)					*	
ENSDARG00000101062	Farnesyl-diphosphate farnesyltransferase 1 (fdft1)					*	*
ENSDARG00000004130	Mevalonate kinase (mvk)					*	*
ENSDARG00000044642	Sterol-C5-desaturase (sc5d)					*	*
ENSDARG00000040890	Farnesyl diphosphate synthase (fdps)					*	
ENSDARG00000103226	7-dehydrocholesterol reductase (dhcr7)					*	*
ENSDARG00000019976	Isopentenyl-diphosphate delta isomerase 1 (idi1)					*	
ENSDARG00000103025	3-hydroxy-3-methylglutaryl-CoA synthase 1 (hmgcs1)					*	*

IPA Canonical Pathways Triacylglycerol Biosynthesis

Zebrafish Gene ID	Gene Name	Molecule ID	P	F1	LRT P	LRT F1	LRT P+F1
ENSDARG00000019897	glycerol-3-phosphate acyltransferase 4	GPAT4		-1.46			
ENSDARG00000011506	lysophosphatidylcholine acyltransferase 1	LPCAT1		-3.15			
ENSDARG00000035028	lysophosphatidylcholine acyltransferase 4	LPCAT4		-3.43			
ENSDARG00000042551	membrane bound O-acyltransferase domain containing 2	MBOAT2		-2.89		*	*
ENSDARG00000102963	sirtuin 6	SIRT6		-1.53			

IPA Top Toxicity List Fatty Acid Metabolism

Zebrafish Gene ID	Gene Name	Molecule ID	P	F1	LRT P	LRT F1	LRT P+F1
ENSDARG00000087262	alcohol dehydrogenase 5 (class III), chi polypeptide	ADH5				*	
ENSDARG00000037873	cytochrome P450 family 3 subfamily A member 7	CYP3A7				*	
ENSDARG00000003854	acyl-CoA synthetase long chain family member 1	ACSL1			*		
ENSDARG00000076780	acyl-CoA dehydrogenase short/branched chain	ACADSB	-8.07		*		
ENSDARG00000043587	steroid 5 alpha-reductase 2	SRD5A2			*		

Figure 5. Transcripts and fold change from selected lipid metabolism pathways. Green cell indicates downregulation and red cell upregulation as compared with the control for at least one generation × treatment comparison based on the Wald test (adjusted $p < 0.05$, $\pm 1 \log_2 \geq$ fold change). Yellow box with an asterisk (*) indicates a transcript that was differentially expressed (adjusted $p < 0.05$) as compared with the control in each likelihood ratio test (LRT) comparison for each generation (P, F1) and across generations (P + F1). Additional tables with fold change information can be found in the online supplemental material Table S8. P = parental; F1 = first filial generation; IPA = Ingenuity Pathway Analysis.

Enrichment of lipid metabolism pathways

As described earlier, the PPAR pathway is essential for regulating energy metabolism and lipid homeostasis; thus, transcriptional dysregulation of the PPAR and associated pathways can result in disruption of lipid metabolism and homeostasis (Grygiel-Górniak, 2014). Corresponding with evidence of transcriptional disruption of PPAR and associated pathways, functional pathways involved in lipid metabolism were significantly enriched in the DAVID pathway and IPA results in response to PFOS exposures in the individual generations (P, F1) and when both generations were combined (P + F1; Tables 3–5, Figure 5). For example, cholesterol biosynthesis pathways were enriched in the Reactome and WikiPathways databases for F1 generation and the combined generations, and steroid biosynthesis was the most enriched KEGG pathway across all comparisons (Table 3, Figure 5, online supplementary material Table S7). Cholesterol biosynthesis pathways were also enriched in the IPA investigation for F1 generation and when both generations were examined together (Table 4). Additionally, the triacylglycerol biosynthesis pathway was significantly enriched in the F1 generation and specifically at the highest PFOS exposure in the F1 generation (Figure 5, online supplementary material Table S8), and the fatty acid metabolism pathway was significantly enriched in the P and F1 generations (Table 5, Figure 5), all indicative of potential impacts of PFOS on lipid metabolism. Finally, pathways involved in bile acid biosynthesis and hepatic cholestasis were significantly enriched in the 101-µg/L PFOS (mea.) treatment in the P generation (Table 4, Figure 4). These results are consistent with previous studies that demonstrated PFOS-induced perturbations in lipid metabolism pathways ranging across multiple vertebrate species (Beale et al., 2022; J. Chen et al., 2014; Christou et al., 2020; Davidsen et al., 2022; G. Dong et al., 2021; Haimbaugh et al., 2022; Jacobsen et al., 2018; H. Lee et al., 2021; Martínez et al., 2019; Mylroie et al., 2021; Rodríguez-Jorquera et al., 2019; Q. Wang et al., 2022).

Although the fatty acid metabolism toxicity pathway was enriched in the P and F1 generations in LRT analyses, the direction of fold change was able to be assessed for only one gene in the P generation, acyl-CoA dehydrogenase short/branched chain (*acadsb*; Figure 5). Acyl-CoA dehydrogenase short/branched chain (*acadsb*) plays an important role in mitochondrial β-oxidation and triglyceride (TG) metabolism (Jiang et al., 2021), and a reduction in *acadsb* expression could represent a decrease in mitochondrial β-oxidation and overall fatty acid metabolism (Ghosh et al., 2016). A reduction in mitochondrial β-oxidation

and subsequent lipid accumulation in the liver has been associated with PFOS exposure in previous studies (Ling et al., 2023; Wan et al., 2012). For the F1 generation, a transcript with homology to the cytochrome P450 family 3 subfamily A (*cyp3c3*) was significantly affected by PFOS exposure. Poly- and perfluoroalkyl substances have been shown to interact directly with CYP3A family molecules, and analysis of human and mouse CYP3A transcripts showed a decrease in expression by animals and cells displaying NAFLD (Woolsey et al., 2015).

For the triacylglycerol biosynthesis pathway, the majority of effects on transcriptional expression occurred in the F1 generation, with the transcripts for the genes *gpat4*, *lpcat1*, *lpcat4*, *mboat2b*, and *sirt6* all significantly decreased as compared with the control (Figure 5). Previous studies in zebrafish have shown that PFOS exposure results in a decrease of TG in the serum and an increase of TG in the liver (Cheng et al., 2016; Y. Cui et al., 2017), and similar increases in TG levels have been observed in livers of mice and chicken embryos (Geng et al., 2019; Huck et al., 2018; Marques et al., 2020). Therefore, with increased incidences of lipid-style hepatocellular vacuolization observed in F1 livers in the present study, concomitant increases in gene expression for TG-related genes were expected; however, the opposite was observed in transcriptomic analysis of F1 liver tissue. This phenomenon has been observed before in a study in Atlantic salmon (*Salmo salar*), where decreases in triacylglyceride synthesis–associated gene expression was seen in salmon livers with higher fat content, potentially exerting negative feedback on triacylglyceride biosynthesis (Horn et al., 2025). Thus, the reduced expression in genes of the triacylglycerol biosynthesis pathway in the present study may also be a result of a similar negative feedback mechanism in the F1 livers.

Cholesterol biosynthesis pathways were overrepresented, where numerous genes within the pathway had significantly affected expression based on LRT analyses (Tables 3–5, Figure 5). However, the direction of fold change was unable to be assessed due to the genes not demonstrating significant DE in any generation × treatment comparison. Nevertheless, perturbances in cholesterol biosynthesis gene expression and total cholesterol (TC) accumulation have been observed in zebrafish and human cell cultures exposed to PFOS (Behr et al., 2020; Cheng et al., 2016; Y. Cui et al., 2017; Louisse et al., 2020; Y. Wang et al., 2020). Louisse et al. (2020), using human HepRG liver cells, observed significantly decreased gene transcript expression in many of the same gene homologues affected in the present study, including *dhcr7*, *ebp*, *fdft1*, *hmgcs1*, *lss*, *scd5*, and *msmo1* (Figure 5, online supplementary material Table S10). It has been hypothesized that since PFOS structurally resembles an unsaturated fatty acid, it may suppress sterol regulatory element-binding proteins in the same manner that the natural ligands do and thus decrease cholesterol biosynthesis pathways (Louisse et al., 2020). Yet, since we cannot conclusively determine the direction of transcriptional disruption observed in the cholesterol biosynthesis pathways in our study, we can only conclude that, like other studies, PFOS exposure results in dysregulation of cholesterol metabolism in zebrafish livers.

Finally, as mentioned previously, genes involved in the bile acid synthesis pathway (*pprc1* and *cyp8b1*) had significantly increased transcriptional expression in the livers of P generation zebrafish in response to PFOS exposure, and PFAS have been shown to perturb bile acid metabolism in in vitro and in vivo studies (Behr et al., 2020; Vujic et al., 2024). Bile acids are regulators of lipid metabolism (J. Liu et al., 2022), and mice fed food supplemented with cholic acid (a bile acid) showed perturbations in gene expression in the TG and cholesterol biosynthesis/homeostasis pathways, as well as differences in TG and TC accumulation in mouse livers (Watanabe et al., 2004). Although *sirt6* did not have the same decreased expression in the P generation as in the F1, it plays an important role in bile acid synthesis, and knockout of the *sirt6* gene in mice has been shown to exacerbate bile acid–related injuries in the liver (X. C. Dong, 2023). Overall, these results highlight that PFOS exposure disrupts transcriptional expression of genes from multiple pathways involved in the delicate regulation of lipid metabolism.

Enrichment of cell cycle pathways and FoxO signaling pathways

Although we have highlighted discrete pathway types and genes thus far in the discussion (PPAR and related pathways, lipid metabolism, and cell cycle pathways), many of these pathways and cellular process controls are interconnected; thus, disruption of the genes in one pathway can have effects on multiple areas of cellular metabolism and regulation (Figure 6, online supplementary material Table S10). In the online supplemental materials, we provide discussion points about observations where PFOS exposure initiated changes in transcriptional expression in zebrafish liver tissues resulting in the significant enrichment of cell cycle pathways and FoxO (forkhead box O) signaling pathways. In that discussion, we provide multiple inferences where these pathways likely have functional impacts connected to perturbed PPAR signaling and lipid metabolism, which may have implications related to cellular proliferation as well as apoptosis.

AOP development

In the present study, we have demonstrated that prolonged PFOS exposures can potentially disrupt the PPAR nuclear signaling pathway (Figure 4), affect transcriptional expression of genes involved in lipid metabolism (Tables 3–5, Figure 5, online supplementary material Table S10), and induce lipid-style hepatocellular vacuolation (Table 1). Ultimately, these observations with parallel observations from the literature suggest mechanistic linkages connecting PFOS exposure through various KEs that can ultimately lead to liver steatosis. Here we have utilized our results and observations gathered from existing literature to develop a formalized AOP outlining how a prototypical xenobiotic stressor (PFOS) binding to PPAR can serve as the MIE for a cascade of KEs involving interference with lipid metabolic processes that ultimately lead to the AO of liver steatosis (Figure 7) with three of the KEs shared with other AOPs related to steatosis. We present a brief outline of the developed AOP and supporting information. The full AOP entry and more detailed information for each KE can be found on the AOP-Wiki site (Society for Advancement of AOPs, 2023) under AOP 529.

Evidence of PFOS/PPAR binding as the MIE

The MIE for this AOP is the binding of a chemical to the PPAR nuclear receptor isoforms. Certain PFAS have structural similarities

KEGG Pathway dre04115:p53 signaling pathway

Gene ID	Gene Name	P	F1	LRT P	LRT F1	LRT P+F1
ENSDARG00000026577	Cyclin dependent kinase 2 (cdk2)		-3.1			
ENSDARG00000075641	STEAP family member 3, metalloreductase (steap3)		2.28		*	
ENSDARG00000009273	Protein phosphatase, Mg2+/Mn2+ dependent, 1Da (ppm1da)		-2.57		*	
ENSDARG00000070012	Sestrin 2 (sesn2)		-2.29		*	
ENSDARG00000079625	ATR serine/threonine kinase (ATR)		-1.88			
ENSDARG00000036180	Cyclin B2 (ccnb2)		-6.51		*	*
ENSDARG00000091926	Caspase 22, apoptosis-related cysteine peptidase (casp22)		3.46			
ENSDARG00000051923	Cyclin B1 (ccnb1)		-6.83		*	*

KEGG Pathway dre04068:FoxO signaling pathway

Gene ID	Gene Name	P	F1	LRT P	LRT F1	LRT P+F1
ENSDARG00000074851	Sphingosine-1-phosphate receptor 4 (s1pr4)	2.3		*		
ENSDARG00000013522	Phosphoenolpyruvate carboxykinase 1 (pck1)			*		
ENSDARG00000016623	Si:ch211-195b13.1			*		
ENSDARG00000042667	Kruppel like factor 2a (klf2a)	2.44		*		
ENSDARG00000029018	Cyclin dependent kinase inhibitor 1Ba (cdkn1ba)			*		*
ENSDARG00000010789	Homer scaffold protein 3b (homer3b)			*		
ENSDARG00000042904	Forkhead box O3b (foxo3b)	2.88		*		
ENSDARG00000063370	Serum/glucocorticoid regulated kinase 2a (sgk2a)		2.75	*		

Reactome R-DRE-69620~Cell Cycle Checkpoints

Gene ID	Gene Name	P	F1	LRT P	LRT F1	LRT P+F1
ENSDARG00000074730	Protein kinase, membrane associated tyrosine/threonine 1 (pkmyt1)					*
ENSDARG00000010792	Cell division cycle 25B (cdc25b)		-3.3		*	*
ENSDARG00000078825	BUB1 mitotic checkpoint serine/threonine kinase Ba (bub1ba)		-4.07		*	*
ENSDARG00000077029	BUB1 mitotic checkpoint serine/threonine kinase (bub1)		-4.49		*	*
ENSDARG00000102674	Cytoskeleton associated protein 5 (ckap5)		-1.75		*	*
ENSDARG00000045951	K(lysine) acetyltransferase 5b (kat5b)					*
ENSDARG00000093313	Ubiquitin B (ubb)	7.38				*
ENSDARG00000043137	Cell division cycle associated 8 (cdca8)		-4.5		*	*
ENSDARG00000063385	Centromere protein E (cenpe)		-4.58		*	*
ENSDARG00000033852	Mitotic arrest deficient 1 like 1 (mad1l1)		-1.54		*	*
ENSDARG00000100741	Cell division cycle 20 homolog (cdc20)		-6.25		*	*
ENSDARG00000040559	RAD1 homolog (rad1)		-2.76		*	*

Figure 6. Transcripts and fold change from selected cell cycle pathways. Green cell indicates downregulation and red cell upregulation as compared with the control for at least one generation × treatment comparison based on the Wald test (adjusted $p < 0.05$, $\pm 1 \log_2 \geq$ fold change). Yellow box with an asterisk (*) indicates a transcript that was differentially expressed (adjusted $p < 0.05$) as compared with the control in each likelihood ratio test (LRT) comparison for each generation (P, F1) and across generations (P + F1). Additional tables with fold change information can be found in online supplementary material Table S8. P = parental; F1 = first filial generation; FoxO = forkhead box O; KEGG = Kyoto Encyclopedia of Genes and Genomes.

to fatty acids, including those with a hydrophilic head group connected to a long linear carbon chain, although the carbons are saturated with fluorine instead of hydrogen. These chemical structures have binding affinity for lipid-binding sites that affect PPAR signaling proteins. Binding analyses and molecular docking models have shown that PFOS and other PFAS can bind to this ligand-binding site of PPARs in the agonist and antagonistic confirmations of the PPARs (Almeida et al., 2021; Garoche et al., 2021; J. Huang, Wang, et al., 2022; Khazaee et al., 2021; Kowalska et al., 2023; Li et al., 2018; P. Wang et al., 2022; Q. Wang et al., 2022; Yi et al., 2019). Beyond binding assays, activity assays in in vitro mammalian cell assays have demonstrated activation of PPAR signaling by PFOS (Behr et al., 2020; Evans et al., 2022; X. Sun et al., 2023; Takacs & Abbott, 2007; Vanden Heuvel et al., 2006; Wolf et al., 2008), and omics studies across multiple vertebrate species have identified PPAR receptors as key molecular targets of PFAS (Beale et al., 2022). Furthermore, PPARα has been demonstrated to have a high degree of conservation among vertebrate species, including mammals, birds, reptiles, amphibians, and fish (Gust et al., 2020), which indicates that the MIE is likely to be conserved among vertebrate species as an overall phylogenetic group.

Disruption of PPAR nuclear signaling (KE1)

The MIE induces KE1 where PPAR nuclear signaling is disrupted. Perfluorooctanesulfonic acid binding to PPAR isoforms has been demonstrated to induce KE1 and have direct effects on the transcriptional expression of the PPAR isoforms, including PPARα and PPARγ in vertebrates (Beale et al., 2022; J. W. Lee et al., 2020). In vitro and in vivo investigations across various terrestrial and aquatic vertebrate species have shown increased or decreased PPAR transcriptional expression depending on species

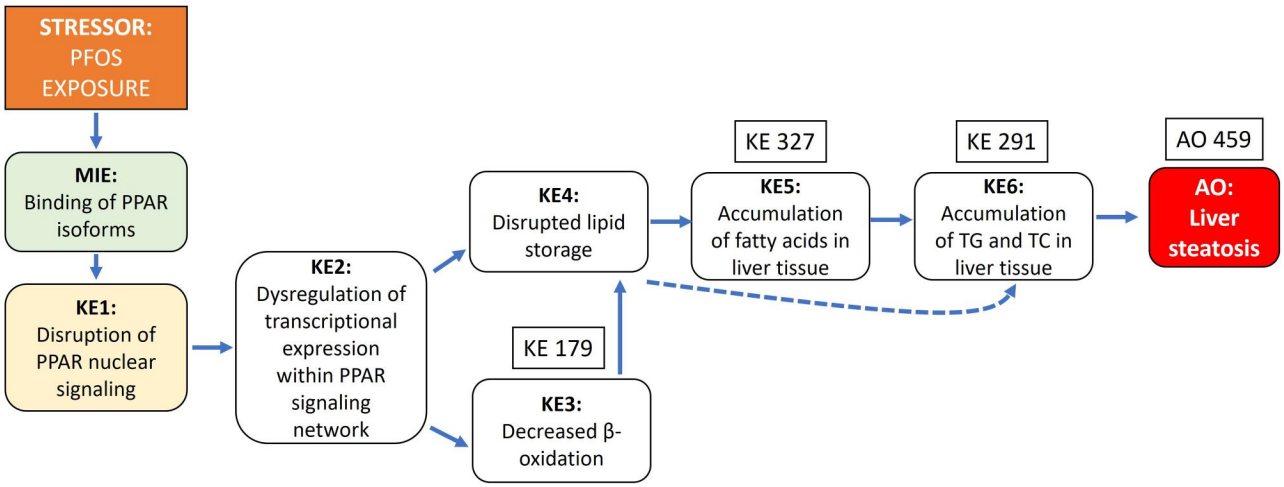

Figure 7. Graphical representation of AOP 529: "Xenobiotic binding to peroxisome proliferator–activated receptors (PPARs) causes dysregulation of lipid metabolism leading to liver steatosis." AOP = adverse outcome pathway; PFOS = perfluorooctanesulfonic acid; MIE = molecular initiating event; KE = key event; TG = triglyceride; TC = total cholesterol; AO = adverse outcome.

(Arukwe & Mortensen, 2011; Christou et al., 2020; Das et al., 2017; Huck et al., 2018; S. Liu et al., 2019; Mylroie et al., 2021; Olivares-Rubio & Vega-López, 2016; Sant et al., 2021; P. Wang et al., 2022). Finally, studies in zebrafish have indicated that modulation of PPAR isoform signaling by PPAR agonist and antagonist resulted in increased lipid accumulation, similar to that seen as a result of PFOS and other PFAS exposures (Venezia et al., 2021). Given the sum of these observations, it is reasonable to hypothesize that PFAS such as PFOS can directly interact with PPARs through receptor binding and thus affect the downstream transcriptional signaling cascade.

Dysregulation of transcriptional expression within the PPAR signaling network (KE2)

Evidence of the overall dysregulation of transcriptional expression within the PPAR signaling network (KE2) has been observed in global and pathway-centered gene expression analyses in embryo and adult zebrafish exposures to PFOS performed in the present study (Figure 4) and our previous research (Mylroie et al., 2021). Pathway and Gene Ontology enrichment analyses from other studies have also identified transcriptional expression underlying lipid metabolism, lipid transport, fatty acid degradation, PPAR signaling, and lipid homeostasis pathways affected by PFOS and other PFAS exposures (Beale et al., 2022; J. Chen et al., 2014; Christou et al., 2020; Davidsen et al., 2022; G. Dong et al., 2021; Haimbaugh et al., 2022; Jacobsen et al., 2018; H. Lee et al., 2021; Martínez et al., 2019; Rodríguez-Jorquera et al., 2019; P. Wang et al., 2022). In the present study, *pprc1* and *tfeb*, which interact with PPARα, were differentially expressed in liver tissue in response to PFOS exposure.

In addition to observations of dysregulation in transcriptional expression of the PPAR receptors, there is ample evidence that PFOS exposure results in transcriptional expression changes in downstream genes involved in the specific process of fatty acid metabolism, lipid storage, and lipid transport. For example, in the present study (Figure 4 and Figure 5, see online supplemental material Table S4) and our previous research (Mylroie et al., 2021), dysregulation of genes related to β-oxidation such as, *cyp8b1*, *acsl1 acox1*, *cpt1ab*, *acadsb*, and *acadm* was observed, similar to in vivo and in vitro studies of vertebrate species including rats, mice, chicken, and zebrafish (Cheng et al., 2016; Dale et al., 2022; Davidsen et al., 2022; Geng et al., 2019; Rosen et al., 2010; Tu et al., 2019; Wan et al., 2012; P. Wang et al., 2022; Yi et al., 2019).

Disruption of transcriptional expression for genes involved in lipid storage, lipogenesis, and lipid transport has been observed across multiple studies (Y. Cui et al., 2017; Huck et al., 2018; S. Liu et al., 2019; Louisse et al., 2020; Martínez et al., 2019; Tse et al., 2016; P. Wang et al., 2022; Yi et al., 2019). For example, disruption in expression of genes such as *acacb*, *apoa*, *apoa2*, and *apoe* and the perilipin (*Plin*) family of genes—which are critical in the storage of lipids, the formation and degradation of lipid droplets, and the regulation of lipid synthesis—has been observed in mice, zebrafish, and fathead minnows after exposure to PFOS (Huck et al., 2018; S. Liu et al., 2019; Louisse et al., 2020; Rodríguez-Jorquera et al., 2019; Tse et al., 2016; P. Wang et al., 2022; Yi et al., 2019; Figure 4). Correspondingly, disruption of *apoa1a* gene expression was observed in the present study. Changes in the expression of these genes has been associated with a shift to accumulation of lipid in hepatocytes and with increased risk of liver steatosis (Carr & Ahima, 2016; Karavia et al., 2012).

Finally, previous work has demonstrated that PFOS exposure can result in transcriptional changes to lipid transport genes in terrestrial vertebrates and fish (Cheng et al., 2016; Christou et al., 2020; Y. Cui et al., 2017; Davidsen et al., 2022; Martínez et al., 2019; Mylroie et al., 2021; Rodríguez-Jorquera et al., 2019; Sant et al., 2021; Tse et al., 2016; P. Wang et al., 2022). Studies in mice (Huck et al., 2018; S. Liu et al., 2019), rats (Davidsen et al., 2022), and human cells (Wan et al., 2012) exposed to PFOS showed increased expression in *CD36*, which is responsible for transport of lipids in liver cells, and such increases in expression have been linked to increased TG levels in the liver (Jia et al., 2023). Altered transcriptional expression of *fabp* isoforms, which

are responsible for the transport of fatty acids as substrates for β-oxidation and lipogenesis, was observed in the present study (Figure 4) and in other studies involving mammals and fish exposed to PFOS (Jacobsen et al., 2018; Mylroie et al., 2021; Rosen et al., 2010; Sant et al., 2021; P. Wang et al., 2022). Furthermore, *lpl*, which enables TG transport, was dysregulated in studies in human cells (Wan et al., 2012), mice (S. Liu et al., 2019), and zebrafish (Cheng et al., 2016; Tse et al., 2016) following PFOS exposure.

Overall, the results from these transcriptional studies show that PFOS exposure caused various disruptions of gene transcript expression within the PPAR nuclear signaling network, including genes involved in fundamental processes that control lipid homeostasis and lipid profiles in liver tissue. Furthermore, evidence for these KEs spans multiple vertebrate species suggesting conservation of responses throughout vertebrates as a phylogenetic group.

Decreased lipid β-oxidation (KE3)

The KE3, decreased lipid β-oxidation, results from the cascade of KE relationships where impacts on KE1 and KE2 ultimately control lipid β-oxidation (Cherkaoui-Malki et al., 2012). For example, decreased lipid β-oxidation has been observed in PPARα knockouts in mice, causing lipid accumulation in the liver (Badman et al., 2007; Hashimoto et al., 2000; Reddy, 2001), whereas stimulation of PPARα increases lipid β-oxidation (Tahri-Joutey et al., 2021). Additionally, PPARβ/δ regulates lipid β-oxidation as demonstrated by Roberts et al. (2011) in a study in live mice and mouse adipocytes where a PPARβ/δ agonist (GW610742) was shown to increase fatty acid β-oxidation. In response to PFOS exposure, Wan et al. (2012) demonstrated that lipid β-oxidation rates were decreased in livers of exposed mice. Exposure to the PFAS perfluorodecanoic acid was also shown to directly reduce lipid β-oxidation in zebrafish embryos (Widhalm et al., 2025). Overall, these results indicate that exposure to PFAS, specifically PFOS, can decreased lipid β-oxidation via disruption of PPAR signaling.

Disrupted lipid storage in the liver (KE4)

Impacts on PPAR signaling have been observed to lead to KE4, disrupted lipid storage (Dixon et al., 2021). The overexpression of PPARγ in mice promotes lipid storage in the liver and thus exacerbates hepatic steatosis (Patsouris et al., 2006; Yu et al., 2003). Conversely, PPARα knockout in mice caused increased lipid deposition in the liver (Patsouris et al., 2006). Y. X. Wang et al. (2003) demonstrated that PPARβ/δ–deficient mice had increased obesity that, while potentially not a function of improper lipid storage, underpins the importance of all PPAR isoforms in proper lipid homeostasis. Moreover, PPARγ agonists can induce increased *cd36* expression (Miao et al., 2022), and increased expression of the fatty acid transport protein CD36 in mice resulted in increased levels of TG in the liver (Koonen et al., 2007). In contrast, genetic deletion of CD36 protein (*cd36*) in mice resulted in lower fatty acid content in livers (Wilson et al., 2016).

Fatty acid–binding proteins deliver fatty acids or other ligands to PPARs, which can then result in the increased expression of gene expression of target FABP genes, suggesting a feedback loop between FABP and PPAR isoforms (Goto et al., 2013; Hotamisligil & Bernlohr, 2015; Morgan et al., 2010). Knockout of the liver FABP in mice resulted in reduced levels of fatty acids in the liver and a reduced uptake of some fatty acids (Newberry et al., 2003). In contrast, induced expression of liver FABP in mouse liver cells resulted in increased TG and TC levels (A. Chen et al., 2013). Peroxisome proliferator–activated receptors also influence the expression of perilipins, which are integral in lipid droplet formation and the storage of TG (Arimura et al., 2004; Takahashi et al., 2013). For example, in perilipin 2 (*plin2*) null mice, TG levels were reduced in the liver as compared with controls (Tsai et al., 2017), and *plin5* null mice showed reductions of TG levels in hepatocytes as compared with wild type mice (Mass-Sanchez et al., 2024). Finally, in exposures based on intestinal organoid models, W. Zhang et al. (2024) found that PFOS exposure stimulated uptake of a fatty acid analogue and increased expression of genes involved in fatty acid transport and lipid droplet synthesis. In response to PFOS exposure in mice, Pfohl et al. (2020) observed increased expression of *Pparα* and *Pparγ* with increased expression of genes and proteins involved in fatty acid transport and storage, which are regulated by PPAR activity. These expression alterations corresponded with decreases in serum TG and TC, suggesting potential alterations in lipid storage and transport. Overall, these lines of evidence provide plausible connection of KE2 and KE3 to lipid storage processes, where PFAS exposures affect these upstream processes ultimately causing KE4, disrupted lipid storage.

Accumulation of fatty acid in livers (KE5)

Decreased lipid β-oxidation (KE3) and subsequent impacts on lipid storage (KE4) can lead to KE5, the accumulation of fatty acids in liver tissue. An investigation of *Pparα*-null mice demonstrated increased fatty acid accumulation during fasting and under normal dietary conditions where these mice were not able to properly catabolize fatty acids even during a bioenergetic deficit (Montagner et al., 2016). Mice exposed to a PFAS mixture similarly showed increased accumulation of fatty acids and changed fatty acid profiles relative to controls, likely initiated via interference with PPAR signaling (Khan et al., 2023). Zebrafish exposed to PFOS also had increased accumulation of fatty acids and changes in fatty acid ratios (Sant et al., 2021).

Accumulation of TG and TC in livers (KE6)

Disruption of proper PPAR signaling can result in an increase in fatty acids in the liver (KE5). In mammals and fish, an excess of fatty acid accumulation in the liver, through excess food uptake or disruption of normal lipid metabolism, results in the liver storing these excesses as lipid droplets made of TG and cholesterol resulting in KE6, the accumulation of TG and TCs in liver (Alves-Bezerra & Cohen, 2017; Ge et al., 2023; Xie et al., 2002). A review by Y. Wang et al. (2020) explains how increased PPARγ expression can alter triacylglycerol levels by increasing expression of genes related to lipid uptake, TG storage, and lipid droplet formation. Investigations across a range of vertebrate species identified that PFOS exposures generally decreased TG and TC in blood/serum (Cheng et al., 2016; Y. Cui et al., 2017; Ho et al., 2022), whereas each was increased in liver tissues and cells (Geng et al., 2019; Huck et al., 2018; Louisse et al., 2020; Liu et al., 2019; Wan et al., 2012; P. Wang et al., 2022). This observation suggests that PFOS exposure causes dysregulation of

systemic lipid homeostasis weighted toward deposition of TC and TG in liver tissues.

Liver steatosis AO

The contribution of fatty acid accumulation (KE5) in addition to TG and TC accumulation (KE6) in liver tissues plausibly contributes to lipid-induced hepatocellular vacuolation, as observed in various vertebrate species exposed to PFOS and other PFAS (Beale et al., 2022; J. W. Lee et al., 2020). Furthermore, there is significant evidence in the literature demonstrating that repression, overexpression, or complete knockout of the various PPAR isoforms can lead to disruptions in lipid metabolism and the AO of liver steatosis. In an extensive review, Y. Wang et al. (2020) presented evidence of how differential repression or activation of the various PPAR isoforms can affect metabolic regulation in mice livers and could lead to lipid accumulation and steatosis in the liver. The present study demonstrated increased incidences of lipid-style hepatocellular vacuolation in the livers of adult zebrafish exposed continuously to PFOS over two 180-day generations (Table 1, Figure 1). Numerous other studies in zebrafish have shown that increased lipid accumulation and/or hepatocellular vacuolation occurs in the developing liver of PFOS-exposed zebrafish beginning at the embryo/larval stage (Sant et al., 2021; Tse et al., 2016; Yi et al., 2019), and other studies report similar outcomes at differing concentrations of PFOS exposure (Cheng et al., 2016; Y. Cui et al., 2017; Du et al., 2009; J. Huang, Liu, et al., 2022; Keiter et al., 2012; P. Wang et al., 2022). Mammalian studies demonstrated PFOS exposures causing lipid accumulation, lipid-style hepatocellular vacuolation, and/or liver steatosis (L. Cui et al., 2009; Davidsen et al., 2022; Huck et al., 2018; Rosen et al., 2010; Salter et al., 2021; L. Zhang et al., 2016). Overall, PPAR represents a critical regulator of the processes leading to the AO of liver steatosis, and the lines of evidence provided within the present body of work demonstrate a logical pathway by which the prototypical stressor, PFOS, binding to PPAR is the MIE for a progression of KEs describing the nuclear signaling, gene expression, metabolic processes, and tissue responses ultimately leading to the AO of liver steatosis.

Note on zebrafish sex

While this study focused on male zebrafish, we ultimately expect similar mechanistic effects in female zebrafish exposed to PFOS based on evidence from the literature and commonalities in metabolism between sexes. Gust et al. (2025) and other studies have shown that male zebrafish bioaccumulate more PFOS than females in equivalent exposures; therefore, male zebrafish likely manifest effects at lower PFOS exposure concentrations than females, although the effects in liver tissue are expected to become similar when tissue concentrations are equivalent.

Conclusions

Results presented herein from liver tissues collected from the first two generations (P and F1) of a three-generation continuous exposure of zebrafish to PFOS provided a unique opportunity to understand the potential multigenerational hepatoxicity of PFOS. Transcriptional effects on PPAR signaling and lipid metabolic pathways provide mechanistic insights into observations of lipid-style hepatocellular vacuolation occurring in male zebrafish exposed at the highest PFOS exposed concentration (100 µg/L, nom.). Of particular note, the scale of effects on the transcriptional responses and the severity of lipid-style hepatocellular vacuolation were greater in the second generation (F1) relative to the first (P). This observation indicates that multigenerational exposures to PFOS may result in more severe impacts in organisms spanning two generations. Finally, these results helped complement and inform the development of the AOP that provides plausible linkage of a prototypical stressor such as PFOS binding to PPAR representing an MIE and a progression of sequential KEs, ultimately culminating with the AO of liver steatosis.

Supplementary material

Supplementary material is available at *Environmental Toxicology and Chemistry* online.

Data availability

The raw RNA sequencing data underlying this article are available at BioProject at https://www.ncbi.nlm.nih.gov/bioproject and accessed with the ID PRJNA1299447. All other data underlying this article will be shared on a reasonable request to the corresponding author.

Author contributions

J. Erik Mylroie (Conceptualization, Data curation, Formal analysis, Funding acquisition, Investigation, Methodology, Project administration, Writing—original draft, Writing—review & editing), Kurt A. Gust (Conceptualization, Data curation, Formal analysis, Funding acquisition, Investigation, Methodology, Project administration, Supervision, Validation, Visualization, Writing—original draft, Writing—review & editing), Chad Blanksma (Data curation, Formal analysis, Investigation, Methodology, Writing—original draft, Writing—review & editing), Alexander B. Lawrence (Data curation, Formal analysis, Writing—review & editing), Allison Hoke (Methodology, Writing—review & editing), Ida Nela Crespo Rosales (Methodology, Writing—review & editing), Mitchell S. Wilbanks (Data curation, Formal analysis, Investigation, Methodology, Validation, Writing—review & editing), Catherine S.C. Steward (Investigation, Methodology, Writing—review & editing), Natàlia Garcia-Reyero (Conceptualization, Funding acquisition, Methodology, Project administration, Supervision, Writing—review & editing), Aarti Gautam (Project administration, Writing—review & editing), Rasha Hammamieh (Project administration, Writing—review & editing), and David W. Moore (Conceptualization, Funding acquisition, Investigation, Project administration, Validation, Writing—original draft, Writing—review & editing)

Funding

This research was funded by the Strategic Environmental Research and Development Program (Project ER20-1542). Zebrafish tissue samples were provided from the Gust et al.

(2024) study, which was funded by select members of the Sediment Management Working Group with supplemental funding from the Strategic Environmental Research and Development Program (Project ER20-1542).

Conflicts of interest

The authors declare no conflict of interest.

Ethical statement

All animal testing was conducted using methods and protocols approved by the Engineer Research and Development Center's Institutional Animal Care and Use Committee of the U.S. Army (Protocol EL-6008-2020-1).

Acknowledgments

The authors would like to thank J. Boyda, N. Barker, K. Chapman, and E. Cowan for assistance with tissue collection and processing and S. Kannan for assistance with uploading raw sequencing reads to the Sequence Read Archive.

References

Agency for Toxic Substances and Disease Registry. (2021). *Toxicological profile for perfluoroalkyls*. US Department of Health and Human Services.

Agrawal, A., Balcı, H., Hanspers, K., Coort, S. L., Martens, M., Slenter, D. N., Ehrhart, F., Digles, D., Waagmeester, A., Wassink, I., Abbassi-Daloii, T., Lopes, E. N., Iyer, A., Acosta, J. M., Willighagen, L. G., Nishida, K., Riutta, A., Basaric, H., Evelo, C. T., … Pico, A. R. (2024). WikiPathways 2024: Next generation pathway database. *Nucleic Acids Research*, *52*, D679–D689. https://doi.org/10.1093/nar/gkad960

Albers, J., Mylroie, J., Kimble, A., Steward, C., Chapman, K., Wilbanks, M., Perkins, E., & Garcia-Reyero, N. (2024). Per- and polyfluoroalkyl substances: Impacts on morphology, behavior and lipid levels in zebrafish embryos. *Toxics*, *12*, 192. https://doi.org/10.3390/toxics12030192

Almeida, N. M., Eken, Y., & Wilson, A. K. (2021). Binding of per- and polyfluoro-alkyl substances to peroxisome proliferator–activated receptor gamma. *ACS Omega*, *6*, 15103–15114. https://doi.org/10.1021/acsomega.1c01304

Alves-Bezerra, M., & Cohen, D. E. (2017). Triglyceride metabolism in the liver. *Comprehensive Physiology*, *8*, 1–8. https://doi.org/10.1002/j.2040-4603.2018.tb00008.x

Andrews, S. (2017, August). *FastQC: A quality control tool for high throughput sequence data.* https://www.bioinformatics.babraham.ac.uk/projects/fastqc

Ankley, G. T., Cureton, P., Hoke, R. A., Houde, M., Kumar, A., Kurias, J., Lanno, R., McCarthy, C., Newsted, J., Salice, C. J., Sample, B. E., Sepúlveda, M. S., Steevens, J., & Valsecchi, S. (2021). Assessing the ecological risks of per- and polyfluoroalkyl substances: Current state-of-the science and a proposed path forward. *Environmental Toxicology and Chemistry*, *40*, 564–605. https://doi.org/10.1002/etc.4869

Annunziato, K. M., Doherty, J., Lee, J., Clark, J. M., Liang, W., Clark, C. W., Nguyen, M., Roy, M. A., & Timme-Laragy, A. R. (2020). Chemical characterization of a legacy aqueous film-forming foam sample and developmental toxicity in zebrafish (*Danio rerio*). *Environmental Health Perspectives*, *128*, 97006. https://doi.org/10.1289/EHP6470

Arimura, N., Horiba, T., Imagawa, M., Shimizu, M., & Sato, R. (2004). The peroxisome proliferator–activated receptor γ regulates expression of the perilipin gene in adipocytes. *The Journal of Biological Chemistry*, *279*, 10070–10076. https://doi.org/10.1074/jbc.M308522200

Arukwe, A., & Mortensen, A. S. (2011). Lipid peroxidation and oxidative stress responses of salmon fed a diet containing perfluorooctane sulfonic- or perfluorooctane carboxylic acids. *Comparative Biochemistry and Physiology Part C: Toxicology & Pharmacology*, *154*, 288–295. https://doi.org/10.1016/j.cbpc.2011.06.012

Badman, M. K., Pissios, P., Kennedy, A. R., Koukos, G., Flier, J. S., & Maratos-Flier, E. (2007). Hepatic fibroblast growth factor 21 is regulated by PPARα and is a key mediator of hepatic lipid metabolism in ketotic states. *Cell Metabolism*, *5*, 426–437. https://doi.org/10.1016/j.cmet.2007.05.002

Beale, D. J., Sinclair, G., Shah, R., Paten, A., Kumar, A., Long, S. M., Vardy, S., & Jones, O. A. (2022). A review of omics-based PFAS exposure studies reveals common biochemical response pathways. *Science of the Total Environment*, *845*, 157255. https://doi.org/10.1016/j.scitotenv.2022.157255

Behr, A. C., Kwiatkowski, A., Ståhlman, M., Schmidt, F. F., Luckert, C., Braeuning, A., & Buhrke, T. (2020). Impairment of bile acid metabolism by perfluorooctanoic acid (PFOA) and perfluorooctanesulfonic acid (PFOS) in human HepaRG hepatoma cells. *Archives of Toxicology*, *94*, 1673–1686. https://doi.org/10.1007/s00204-020-02732-3

Bell, E. M., De Guise, S., McCutcheon, J. R., Lei, Y., Levin, M., Li, B., Rusling, J. F., Lawrence, D. A., Cavallari, J. M., O'Connell, C., Javidi, B., Wang, X., & Ryu, H. (2021). Exposure, health effects, sensing, and remediation of the emerging PFAS contaminants—Scientific challenges and potential research directions. *The Science of the Total Environment*, *780*, 146399. https://doi.org/10.1016/j.scitotenv.2021.146399

Bolger, A. M., Lohse, M., & Usadel, B. (2014). Trimmomatic: A flexible trimmer for Illumina sequence data. *Bioinformatics*, *30*, 2114–2120. https://doi.org/10.1093/bioinformatics/btu170http://www.usadellab.org/cms/? page=trimmomatic.

Boyd, R. I., Ahmad, S., Singh, R., Fazal, Z., Prins, G. S., Madak Erdogan, Z., Irudayaraj, J., & Spinella, M. J. (2022). Toward a mechanistic understanding of poly- and perfluoroalkylated substances and cancer. *Cancers*, *14*, 2919. https://doi.org/10.3390/cancers14122919

Carr, R. M., & Ahima, R. S. (2016). Pathophysiology of lipid droplet proteins in liver diseases. *Experimental Cell Research*, *340*, 187–192. https://doi.org/10.1016/j.yexcr.2015.10.021

Carson, F. L., & Hladik, C. (1997). *Histotechnology: A self-instructional text*. ASCP Press.

Chang, E. T., Adami, H. O., Boffetta, P., Cole, P., Starr, T. B., & Mandel, J. S. (2014). A critical review of perfluorooctanoate and perfluorooctanesulfonate exposure and cancer risk in humans. *Critical Reviews in Toxicology*, *44 (Suppl. 1)*, 1–81. https://doi.org/10.3109/10408444.2014.905767

Chao, X., Wang, S., Zhao, K., Li, Y., Williams, J. A., Li, T., Chavan, H., Krishnamurthy, P., He, X. C., Li, L., Ballabio, A., Ni, H.-M., & Ding, W.-X. (2018). Impaired TFEB-mediated lysosome biogenesis and autophagy promote chronic ethanol-induced liver injury and steatosis in mice. *Gastroenterology*, *155*, 865–879. e12. https://doi.org/10.1053/j.gastro.2018.05.027

Chen, A., Tang, Y., Davis, V., Hsu, F. F., Kennedy, S. M., Song, H., Turk, J., Brunt, E. M., Newberry, E. P., & Davidson, N. O. (2013). Liver fatty acid binding protein (L-Fabp) modulates murine stellate cell activation and diet-induced nonalcoholic fatty liver disease. *Hepatology*, *57*, 2202–2212. https://doi.org/10.1002/hep.26318

Chen, J., Tanguay, R. L., Tal, T. L., Gai, Z., Ma, X., Bai, C., Tilton, S. C., Jin, D., Yang, D., Huang, C., & Dong, Q. (2014). Early life perfluorooctanesulphonic acid (PFOS) exposure impairs zebrafish organogenesis. *Aquatic Toxicology*, *150*, 124–132. https://doi.org/10.1016/j.aquatox.2014.03.005

Cheng, J., Lv, S., Nie, S., Liu, J., Tong, S., Kang, N., Xiao, Y., Dong, Q., Huang, C., & Yang, D. (2016). Chronic perfluorooctane sulfonate (PFOS) exposure induces hepatic steatosis in zebrafish. *Aquatic Toxicology*, *176*, 45–52. https://doi.org/10.1016/j.aquatox.2016.04.013

Cherkaoui-Malki, M., Surapureddi, S., El Hajj, H. I., Vamecq, J., & Andreoletti, P. (2012). Hepatic steatosis and peroxisomal fatty acid beta-oxidation. *Current Drug Metabolism*, *13*, 1412–1421. https://doi.org/10.2174/138920012803762765

Christou, M., Fraser, T. W., Berg, V., Ropstad, E., & Kamstra, J. H. (2020). Calcium signaling as a possible mechanism behind increased locomotor response in zebrafish larvae exposed to a human relevant persistent organic pollutant mixture or PFOS. *Environmental Research*, *187*, 109702. https://doi.org/10.1016/j.envres.2020.109702

Costello, E., Rock, S., Stratakis, N., Eckel, S. P., Walker, D. I., Valvi, D., Cserbik, D., Jenkins, T., Xanthakos, S. A., Kohli, R., Sisley, S., Vasiliou, V., La Merrill, M. A., Rosen, H., Conti, D. V., McConnell, R., & Chatzi, L. (2022). Exposure to per- and polyfluoroalkyl substances and markers of liver injury: A systematic review and meta-analysis. *Environmental Health Perspectives*, *130*, 46001. https://doi.org/10.1289/EHP10092

Crissman, J. W., Goodman, D. G., Hildebrandt, P. K., Maronpot, R. R., Prater, D. A., Riley, J. H., Seaman, W. J., & Thake, D. C. (2004). Best practices guideline: Toxicologic histopathology. *Toxicologic Pathology*, *32*, 126–131. https://doi.org/10.1080/01926230490268756

Cui, L., Zhou, Q. F., Liao, C. Y., Fu, J. J., & Jiang, G. B. (2009). Studies on the toxicological effects of PFOA and PFOS on rats using histological observation and chemical analysis. *Archives of Environmental Contamination and Toxicology*, *56*, 338–349. https://doi.org/10.1007/s00244-008-9194-6

Cui, Y., Lv, S., Liu, J., Nie, S., Chen, J., Dong, Q., Huang, C., & Yang, D. (2017). Chronic perfluorooctanesulfonic acid exposure disrupts lipid metabolism in zebrafish. *Human & Experimental Toxicology*, *36*, 207–217. https://doi.org/10.1177/0960327116646615

Dale, K., Yadetie, F., Horvli, T., Zhang, X., Frøysa, H. G., Karlsen, O. A., & Goksøyr, A. (2022). Single PFAS and PFAS mixtures affect nuclear receptor– and oxidative stress–related pathways in precision-cut liver slices of Atlantic cod (*Gadus morhua*). *The Science of the Total Environment*, *814*, 152732. https://doi.org/10.1016/j.scitotenv.2021.152732

Das, K. P., Wood, C. R., Lin, M. T., Starkov, A. A., Lau, C., Wallace, K. B., Corton, J. C., & Abbott, B. D. (2017). Perfluoroalkyl acids-induced liver steatosis: Effects on genes controlling lipid homeostasis. *Toxicology*, *378*, 37–52. https://doi.org/10.1016/j.tox.2016.12.007

Davidsen, N., Ramhøj, L., Lykkebo, C. A., Kugathas, I., Poulsen, R., Rosenmai, A. K., Evrard, B., Darde, T. A., Axelstad, M., Bahl, M. I., Hansen, M., Chalmel, F., Licht, T. R., & Svingen, T. (2022). PFOS-induced thyroid hormone system disrupted rats display organ-specific changes in their transcriptomes. *Environmental Pollution*, *305*, 119340. https://doi.org/10.1016/j.envpol.2022.119340

Denslow, N. D., Chow, M. C., Kroll, K. J., & Green, L. (1999). Vitellogenin as a biomarker of exposure for estrogen or estrogen mimics. *Ecotoxicology*, *8*, 385–398. https://doi.org/10.1023/A:1008986522208

DeWitt, J. C., Blossom, S. J., & Schaider, L. A. (2019). Exposure to per-fluoroalkyl and polyfluoroalkyl substances leads to immunotoxicity: Epidemiological and toxicological evidence. *Journal of Exposure Science & Environmental Epidemiology*, *29*, 148–156. https://doi.org/10.1038/s41370-018-0097-y

Dixon, E. D., Nardo, A. D., Claudel, T., & Trauner, M. (2021). The role of lipid sensing nuclear receptors (PPARs and LXR) and metabolic lipases in obesity, diabetes and NAFLD. *Genes*, *12*, 645. https://doi.org/10.3390/genes12050645

Dobin, A., Davis, C. A., Schlesinger, F., Drenkow, J., Zaleski, C., Jha, S., Batut, P., Chaisson, M., & Gingeras, T. R. (2013). STAR: Ultrafast universal RNA-seq aligner. *Bioinformatics*, *29*, 15–21. https://doi.org/10.1093/bioinformatics/bts635https://github.com/alexdobin/STAR.

Dong, G., Zhang, R., Huang, H., Lu, C., Xia, Y., Wang, X., & Du, G. (2021). Exploration of the developmental toxicity of TCS and PFOS to zebrafish embryos by whole-genome gene expression analyses. *Environmental Science and Pollution Research International*, *28*, 56032–56042. https://doi.org/10.1007/s11356-021-14527-9

Dong, X. C. (2023). Sirtuin 6—A key regulator of hepatic lipid metabolism and liver health. *Cells*, *12*, 663. https://doi.org/10.3390/cells12040663

Du, Y., Shi, X., Liu, C., Yu, K., & Zhou, B. (2009). Chronic effects of water-borne PFOS exposure on growth, survival and hepatotoxicity in zebrafish: A partial life-cycle test. *Chemosphere*, *74*, 723–729. https://doi.org/10.1016/j.chemosphere.2008.09.075

Ducatman, A., & Fenton, S. E. (2022). Invited perspective: PFAS and liver disease: Bringing all the evidence together. *Environmental Health Perspectives*, *130*, 41303. https://doi.org/10.1289/EHP11149

Evans, N., Conley, J. M., Cardon, M., Hartig, P., Medlock-Kakaley, E., & Gray, L. E. Jr, (2022). In vitro activity of a panel of per- and polyfluoroalkyl substances (PFAS), fatty acids, and pharmaceuticals in peroxisome proliferator–activated receptor (PPAR) alpha, PPAR gamma, and estrogen receptor assays. *Toxicology and Applied Pharmacology*, *449*, 116136. https://doi.org/10.1016/j.taap.2022.116136

Fragki, S., Dirven, H., Fletcher, T., Grasl-Kraupp, B., Bjerve Gützkow, K., Hoogenboom, R., Kersten, S., Lindeman, B., Louisse, J., Peijnenburg, A., Piersma, A. H., Princen, H. M. G.,

Uhl, M., Westerhout, J., Zeilmaker, M. J., & Luijten, M. (2021). Systemic PFOS and PFOA exposure and disturbed lipid homeostasis in humans: What do we know and what not? *Critical Reviews in Toxicology*, *51*, 141–164. https://doi.org/10.1080/10408444.2021.1888073

Garoche, C., Boulahtouf, A., Grimaldi, M., Chiavarina, B., Toporova, L., den Broeder, M. J., Legler, J., Bourguet, W., & Balaguer, P. (2021). Interspecies differences in activation of peroxisome proliferator–activated receptor γ by pharmaceutical and environmental chemicals. *Environmental Science & Technology*, *55*, 16489–16501. https://doi.org/10.1021/acs.est.1c04318

Ge, G., Ren, J., Song, G., Li, Q., & Cui, Z. (2023). Transcriptome analysis reveals the molecular basis of overfeeding-induced diabetes in zebrafish. *International Journal of Molecular Sciences*, *24*, 11994. https://doi.org/10.3390/ijms241511994

Geng, D., Musse, A. A., Wigh, V., Carlsson, C., Engwall, M., Orešič, M., Scherbak, N., & Hyötyläinen, T. (2019). Effect of perfluorooctanesulfonic acid (PFOS) on the liver lipid metabolism of the developing chicken embryo. *Ecotoxicology and Environmental Safety*, *170*, 691–698. https://doi.org/10.1016/j.ecoenv.2018.12.040

Ghosh, S., Kruger, C., Wicks, S., Simon, J., Kumar, K. G., Johnson, W. D., Mynatt, R. L., Noland, R. C., & Richards, B. K. (2016). Short chain acyl-CoA dehydrogenase deficiency and short-term high-fat diet perturb mitochondrial energy metabolism and transcriptional control of lipid-handling in liver. *Nutrition & Metabolism*, *13*, 17. https://doi.org/10.1186/s12986-016-0075-0

Glüge, J., Scheringer, M., Cousins, I. T., DeWitt, J. C., Goldenman, G., Herzke, D., Lohmann, R., Ng, C. A., Trier, X., & Wang, Z. (2020). An overview of the uses of per- and polyfluoroalkyl substances (PFAS). *Environmental Science: Processes & Impacts*, *22*, 2345–2373. https://doi.org/10.1039/d0em00291g

Gong, Q., Zhang, X., Sun, Y., Shen, J., Li, X., Xue, C., & Liu, Z. (2022). Transcription factor EB inhibits non-alcoholic fatty liver disease through fibroblast growth factor 21. *Journal of Molecular Medicine*, *100*, 1587–1597. https://doi.org/10.1007/s00109-022-02256-6

Goto, K., Iso, T., Hanaoka, H., Yamaguchi, A., Suga, T., Hattori, A., Irie, Y., Shinagawa, Y., Matsui, H., Syamsunarno, M. R. A. A., Matsui, M., Haque, A., Arai, M., Kunimoto, F., Yokoyama, T., Endo, K., Gonzalez, F. J., & Kurabayashi, M. (2013). Peroxisome proliferator-activated receptor-γ in capillary endothelia promotes fatty acid uptake by heart during long-term fasting. *Journal of the American Heart Association*, *2*, e004861. https://doi.org/10.1161/JAHA.112.004861

Green, J. W., Springer, T. A., Saulnier, A. N., & Swintek, J. (2014). Statistical analysis of histopathological endpoints. *Environmental Toxicology and Chemistry*, *33*, 1108–1116. https://doi.org/10.1002/etc.2530

Grygiel-Górniak, B. (2014). Peroxisome proliferator–activated receptors and their ligands: Nutritional and clinical implications—A review. *Nutrition Journal*, *13*, 17–10. https://doi.org/10.1186/1475-2891-13-17

Gumilas, N. S. A., Harini, I. M., Ernawati, D. A., Indriani, V., Novrial, D., & Kurniawan, D. W. (2022). Potential of apolipoprotein A1 (ApoA1) for detecting liver cirrhosis and hepatocellular carcinoma. *Asian Pacific Journal of Cancer Prevention: APJCP*, *23*, 2001–2008. https://doi.org/10.31557/APJCP.2022.23.6.2001

Gust, K. A., Ji, Q., & Luo, X. (2020). Example of adverse outcome pathway concept enabling genome-to-phenome discovery in toxicology. *Integrative and Comparative Biology*, *60*, 375–384. https://doi.org/10.1093/icb/icaa064

Gust, K. A., Kimble, A. N., Mylroie, J. E., Mayo, M. L., Wilbanks, M. S., Steward, C. S., Chapman, K. A., Lotufo, G. R., Garcia-Reyero, N., & Moore, D. W. (2025). Bioconcentration, maternal transfer, and toxicokinetics of PFOS in a multi-generational zebrafish exposure. *Environmental Toxicology and Chemistry*, *44*, 207–219. https://doi.org/10.1093/etojnl/vgae033

Gust, K. A., Mylroie, J. E., Kimble, A. N., Wilbanks, M. S., Steward, C. S. C., Chapman, K. A., Jensen, K. M., Kennedy, A. J., Krupa, P. M., Waisner, S. A., Pandelides, Z., Garcia-Reyero, N., Erickson, R. J., Ankley, G. T., Conder, J., & Moore, D. W. (2024). Survival, growth, and reproduction responses in a three-generation exposure of the zebrafish (*Danio rerio*) to perfluorooctane sulfonate. *Environmental Toxicology and Chemistry*, *43*, 115–131. https://doi.org/10.1002/etc.5770

Gust, K. A., Wilbanks, M. S., Collier, Z. A., Burgoon, L. D., & Perkins, E. J. (2019). *Adverse outcome pathway on antagonist binding to PPARα leading to body-weight loss*. Organisation for Economic Co-operation and Development.

Haimbaugh, A., Wu, C. C., Akemann, C., Meyer, D. N., Connell, M., Abdi, M., Khalaf, A., Johnson, D., & Baker, T. R. (2022). Multi- and transgenerational effects of developmental exposure to environmental levels of PFAS and PFAS mixture in zebrafish (*Danio rerio*). *Toxics*, *10*, 334. https://doi.org/10.3390/toxics10060334

Harrison, P. W., Amode, M. R., Austine-Orimoloye, O., Azov, A. G., Barba, M., Barnes, I., Becker, A., Bennett, R., Berry, A., Bhai, J., Bhurji, S. K., Boddu, S., Branco Lins, P. R., Brooks, L., Ramaraju, S. B., Campbell, L. I., Martinez, M. C., Charkhchi, M., Chougule, K., … Yates, A. D. (2024). Ensembl 2024. *Nucleic Acids Research*, *52*, D891–D899. https://doi.org/10.1093/nar/gkad1049https://www.ensembl.org.

Hashimoto, T., Cook, W. S., Qi, C., Yeldandi, A. V., Reddy, J. K., & Rao, M. S. (2000). Defect in peroxisome proliferator–activated receptor α-inducible fatty acid oxidation determines the severity of hepatic steatosis in response to fasting. *The Journal of Biological Chemistry*, *275*, 28918–28928. https://doi.org/10.1074/jbc.M910350199

Ho, S. H., Soh, S. X. H., Wang, M. X., Ong, J., Seah, A., Wong, Y., Fang, Z., Sim, S., & Lim, J. T. (2022). Perfluoroalkyl substances and lipid concentrations in the blood: A systematic review of epidemiological studies. *The Science of the Total Environment*, *850*, 158036. https://doi.org/10.1016/j.scitotenv.2022.158036

Horn, S. S., Sonesson, A. K., Krasnov, A., Aslam, M. L., Hillestad, B., & Ruyter, B. (2025). Genetic and metabolic characterization of individual differences in liver fat accumulation in Atlantic salmon. *Frontiers in Genetics*, *16*, 1512769. https://doi.org/10.3389/fgene.2025.1512769

Hotamisligil, G. S., & Bernlohr, D. A. (2015). Metabolic functions of FABPs—Mechanisms and therapeutic implications. *Nature Reviews: Endocrinology*, *11*, 592–605. https://doi.org/10.1038/nrendo.2015.122

Huang, D. W., Sherman, B. T., & Lempicki, R. A. (2009). Systematic and integrative analysis of large gene lists using

DAVID bioinformatics resources. *Nature Protocols*, *4*, 44–57. https://doi.org/10.1038/nprot.2008.211

Huang, J., Liu, Y., Wang, Q., Yi, J., Lai, H., Sun, L., Mennigen, J. A., & Tu, W. (2022). Concentration-dependent toxicokinetics of novel PFOS alternatives and their chronic combined toxicity in adult zebrafish. *The Science of the Total Environment*, *839*, 156388. https://doi.org/10.1016/j.scitotenv.2022.156388

Huang, J., Wang, Q., Liu, S., Lai, H., & Tu, W. (2022). Comparative chronic toxicities of PFOS and its novel alternatives on the immune system associated with intestinal microbiota dysbiosis in adult zebrafish. *Journal of Hazardous Materials*, *425*, 127950. https://doi.org/10.1016/j.jhazmat.2021.127950

Huck, I., Beggs, K., & Apte, U. (2018). Paradoxical protective effect of perfluorooctanesulfonic acid against high-fat diet–induced hepatic steatosis in mice. *International Journal of Toxicology*, *37*, 383–392. https://doi.org/10.1177/1091581818790934

Jacobsen, A. V., Nordén, M., Engwall, M., & Scherbak, N. (2018). Effects of perfluorooctane sulfonate on genes controlling hepatic fatty acid metabolism in livers of chicken embryos. *Environmental Science and Pollution Research International*, *25*, 23074–23081. https://doi.org/10.1007/s11356-018-2358-7

Jia, Y., Zhu, Y., Wang, R., Ye, Q., Xu, D., Zhang, W., Zhang, Y., Shan, G., & Zhu, L. (2023). Novel insights into the mediating roles of cluster of differentiation 36 in transmembrane transport and tissue partition of per- and polyfluoroalkyl substances in mice. *Journal of Hazardous Materials*, *442*, 130129. https://doi.org/10.1016/j.jhazmat.2022.130129

Jiang, P., Iqbal, A., Wang, M., Li, X., Fang, X., Yu, H., & Zhao, Z. (2021). Transcriptomic analysis of short/branched-chain acyl--coenzyme a dehydrogenase knocked out bMECs revealed its regulatory effect on lipid metabolism. *Frontiers in Veterinary Science*, *8*, 744287. https://doi.org/10.3389/fvets.2021.744287

Johnson, R., Wolf, J., & Braunbeck, T. (2009). *OECD guidance document for the diagnosis of endocrine-related histopathology of fish gonads*. Organisation for Economic Co-operation and Development.

Kanehisa, M. (2019). Toward understanding the origin and evolution of cellular organisms. *Protein Science*, *28*, 1947–1951. https://doi.org/10.1002/pro.3715

Kanehisa, M., Furumichi, M., Sato, Y., Kawashima, M., & Ishiguro-Watanabe, M. (2023). KEGG for taxonomy-based analysis of pathways and genomes. *Nucleic Acids Research*, *51*, D587–D592. https://doi.org/10.1093/nar/gkac963

Kanehisa, M., & Goto, S. (2000). KEGG: Kyoto Encyclopedia of Genes and Genomes. *Nucleic Acids Research*, *28*, 27–30. https://doi.org/10.1093/nar/28.1.27https://www.genome.jp/kegg/.

Karavia, E. A., Papachristou, D. J., Liopeta, K., Triantaphyllidou, I. E., Dimitrakopoulos, O., & Kypreos, K. E. (2012). Apolipoprotein AI modulates processes associated with diet-induced nonalcoholic fatty liver disease in mice. *Molecular Medicine*, *18*, 901–912. https://doi.org/10.2119/molmed.2012.00113

Keiter, S., Baumann, L., Färber, H., Holbech, H., Skutlarek, D., Engwall, M., & Braunbeck, T. (2012). Long-term effects of a binary mixture of perfluorooctane sulfonate (PFOS) and bisphenol A (BPA) in zebrafish (*Danio rerio*). *Aquatic Toxicology*, *118–119*, 116–129. https://doi.org/10.1016/j.aquatox.2012.04.003

Kent, M. L., Spitsbergen, J. M., Matthews, J. M., Fournie, J. W., & Westerfield, M. (2012). *Diseases of zebrafish in research facilities*. Zebrafish International Resource Center. https://zebrafish.org/wiki/health/disease_manual/recipes_and_protocols

Khan, E. A., Grønnestad, R., Krøkje, Å., Bartosov, Z., Johanson, S. M., Müller, M. H., & Arukwe, A. (2023). Alteration of hepato-lipidomic homeostasis in A/J mice fed an environmentally relevant PFAS mixture. *Environment International*, *173*, 107838. https://doi.org/10.1016/j.envint.2023.107838

Khazaee, M., Christie, E., Cheng, W., Michalsen, M., Field, J., & Ng, C. (2021). Perfluoroalkyl acid binding with peroxisome proliferator–activated receptors α, γ, and δ, and fatty acid binding proteins by equilibrium dialysis with a comparison of methods. *Toxics*, *9*, 45. https://doi.org/10.3390/toxics9030045

Khazaee, M., Guardian, M. G. E., Aga, D. S., & Ng, C. A. (2020). Impacts of sex and exposure duration on gene expression in zebrafish following perfluorooctane sulfonate exposure. *Environmental Toxicology and Chemistry*, *39*, 437–449. https://doi.org/10.1002/etc.4628

Koonen, D. P., Jacobs, R. L., Febbraio, M., Young, M. E., Soltys, C. L. M., Ong, H., Vance, D. E., & Dyck, J. R. (2007). Increased hepatic CD36 expression contributes to dyslipidemia associated with diet-induced obesity. *Diabetes*, *56*, 2863–2871. https://doi.org/10.2337/db07-0907

Kowalska, D., Sosnowska, A., Bulawska, N., Stępnik, M., Besselink, H., Behnisch, P., & Puzyn, T. (2023). How the structure of per- and polyfluoroalkyl substances (PFAS) influences their binding potency to the peroxisome proliferator–activated and thyroid hormone receptors—An in silico screening study. *Molecules*, *28*, 479. https://doi.org/10.3390/molecules28020479

Krämer, A., Green, J., Pollard, J., Jr,., & Tugendreich, S. (2014). Causal analysis approaches in ingenuity pathway analysis. *Bioinformatics*, *30*, 523–530. https://doi.org/10.1093/bioinformatics/btt703

Kudaravalli, P., & John, S. (2023). *Nonalcoholic fatty liver*. StatPearls Publishing.

Lamas Bervejillo, M., & Ferreira, A. M. (2019). Understanding peroxisome proliferator–activated receptors: From the structure to the regulatory actions on metabolism. *Advances in Experimental Medicine and Biology*, *1127*, 39–57. https://doi.org/10.1007/978-3-030-11488-6_3

Lee, H., Sung, E. J., Seo, S., Min, E. K., Lee, J. Y., Shim, I., Kim, P., Kim, T. Y., Lee, S., & Kim, K. T. (2021). Integrated multi-omics analysis reveals the underlying molecular mechanism for developmental neurotoxicity of perfluorooctanesulfonic acid in zebrafish. *Environment International*, *157*, 106802. https://doi.org/10.1016/j.envint.2021.106802

Lee, J. W., Choi, K., Park, K., Seong, C., Do Yu, S., & Kim, P. (2020). Adverse effects of perfluoroalkyl acids on fish and other aquatic organisms: A review. *The Science of the Total Environment*, *707*, 135334. https://doi.org/10.1016/j.scitotenv.2019.135334

Li, C. H., Ren, X. M., Ruan, T., Cao, L. Y., Xin, Y., Guo, L. H., & Jiang, G. (2018). Chlorinated polyfluorinated ether sulfonates exhibit higher activity toward peroxisome proliferator–activated receptors signaling pathways than perfluorooctanesulfonate. *Environmental Science & Technology*, *52*, 3232–3239. https://doi.org/10.1021/acs.est.7b06327

Lin, H., Wu, H., Liu, F., Yang, H., Shen, L., Chen, J., Zhang, X., Zhong, Y., Zhang, H., & Liu, Z. (2022). Assessing the hepatotoxicity of PFOA, PFOS, and 6:2 Cl-PFESA in black-spotted frogs (*Rana nigromaculata*) and elucidating potential association with gut microbiota. *Environmental Pollution*, *312*, 120029. https://doi.org/10.1016/j.envpol.2022.120029

Ling, J., Hua, L., Qin, Y., Gu, T., Jiang, S., & Zhao, J. (2023). Perfluorooctane sulfonate promotes hepatic lipid accumulation and steatosis in high-fat diet mice through AMP-activated protein kinase/acetyl-CoA carboxylase (AMPK/ACC) pathway. *Journal of Applied Toxicology*, *43*, 312–322. https://doi.org/10.1002/jat.4383

Liu, J., Carlson, H. A., & Scott, E. E. (2022). The structure and characterization of human cytochrome P450 8B1 supports future drug design for nonalcoholic fatty liver disease and diabetes. *Journal of Biological Chemistry*, *298*, 102344. https://doi.org/10.1016/j.jbc.2022.102344

Liu, S., Yang, R., Yin, N., Wang, Y. L., & Faiola, F. (2019). Environmental and human relevant PFOS and PFOA doses alter human mesenchymal stem cell self-renewal, adipogenesis and osteogenesis. *Ecotoxicology and Environmental Safety*, *169*, 564–572. https://doi.org/10.1016/j.ecoenv.2018.11.064

Louisse, J., Rijkers, D., Stoopen, G., Janssen, A., Staats, M., Hoogenboom, R., Kersten, S., & Peijnenburg, A. (2020). Perfluorooctanoic acid (PFOA), perfluorooctane sulfonic acid (PFOS), and perfluorononanoic acid (PFNA) increase triglyceride levels and decrease cholesterogenic gene expression in human HepaRG liver cells. *Archives of Toxicology*, *94*, 3137–3155. https://doi.org/10.1007/s00204-020-02808-0

Love, M. I., Huber, W., & Anders, S. (2014). Moderated estimation of fold change and dispersion for RNA-seq data with DESeq2. *Genome Biology*, *15*, 550. https://doi.org/10.1186/s13059-014-0550-8https://github.com/thelovelab/DESeq2.

Marques, E., Pfohl, M., Auclair, A., Jamwal, R., Barlock, B. J., Sammoura, F. M., Goedken, M., Akhlaghi, F., & Slitt, A. L. (2020). Perfluorooctanesulfonic acid (PFOS) administration shifts the hepatic proteome and augments dietary outcomes related to hepatic steatosis in mice. *Toxicology and Applied Pharmacology*, *408*, 115250. https://doi.org/10.1016/j.taap.2020.115250

Martínez, R., Navarro-Martín, L., Luccarelli, C., Codina, A. E., Raldúa, D., Barata, C., Tauler, R., & Piña, B. (2019). Unravelling the mechanisms of PFOS toxicity by combining morphological and transcriptomic analyses in zebrafish embryos. *The Science of the Total Environment*, *674*, 462–471. https://doi.org/10.1016/j.scitotenv.2019.04.200

Mass-Sanchez, P. B., Krizanac, M., Štancl, P., Leopold, M., Engel, K. M., Buhl, E. M., van Helden, J., Gassler, N., Schiller, J., Karlić, R., Möckel, D., Lammers, T., Meurer, S. K., Weiskirchen, R., & Asimakopoulos, A. (2024). Perilipin 5 deletion protects against nonalcoholic fatty liver disease and hepatocellular carcinoma by modulating lipid metabolism and inflammatory responses. *Cell Death Discovery*, *10*, 94. https://doi.org/10.1038/s41420-024-01860-4

Miao, Y., Zhang, C., Yang, L., Zeng, X., Hu, Y., Xue, X., Dai, Y., & Wei, Z. (2022). The activation of PPARγ enhances Treg responses through up-regulating CD36/CPT1-mediated fatty acid oxidation and subsequent N-glycan branching of TβRII/IL-2Rα. *Cell Communication and Signaling: CCS*, *20*, 48. https://doi.org/10.1186/s12964-022-00849-9

Milacic, M., Beavers, D., Conley, P., Gong, C., Gillespie, M., Griss, J., Haw, R., Jassal, B., Matthews, L., May, B., Petryszak, R., Ragueneau, E., Rothfels, K., Sevilla, C., Shamovsky, V., Stephan, R., Tiwari, K., Varusai, T., Weiser, J., … D'Eustachio, P. (2024). The reactome pathway knowledgebase 2024. *Nucleic Acids Research*, *52*, D672–D678. https://doi.org/10.1093/nar/gkad1025https://reactome.org/,

Miyazaki, H., Sawada, T., Kiyohira, M., Yu, Z., Nakamura, K., Yasumoto, Y., Kagawa, Y., Ebrahimi, M., Islam, A., Sharifi, K., Kawamura, S., Kodama, T., Yamamoto, Y., Adachi, Y., Tokuda, N., Terai, S., Sakaida, I., Ishikawa, T., & Owada, Y. (2014). Fatty acid binding protein 7 regulates phagocytosis and cytokine production in Kupffer cells during liver injury. *The American Journal of Pathology*, *184*, 2505–2515. https://doi.org/10.1016/j.ajpath.2014.05.015

Montagner, A., Polizzi, A., Fouché, E., Ducheix, S., Lippi, Y., Lasserre, F., Barquissau, V., Régnier, M., Lukowicz, C., Benhamed, F., Iroz, A., Bertrand-Michel, J., Al Saati, T., Cano, P., Mselli-Lakhal, L., Mithieux, G., Rajas, F., Lagarrigue, S., Pineau, T., … Guillou, H. (2016). Liver PPARα is crucial for whole-body fatty acid homeostasis and is protective against NAFLD. *Gut*, *65*, 1202–1214. https://doi.org/10.1136/gutjnl-2015-310798

Morgan, E., Kannan-Thulasiraman, P., & Noy, N. (2010). Involvement of fatty acid binding protein 5 and PPARβ/δ in prostate cancer cell growth. *PPAR Research*, *2010*, 234629. https://doi.org/10.1155/2010/234629

Mylroie, J. E., Wilbanks, M. S., Kimble, A. N., To, K. T., Cox, C. S., McLeod, S. J., Gust, K. A., Moore, D. W., Perkins, E. J., & Garcia-Reyero, N. (2021). Perfluorooctanesulfonic acid–induced toxicity on zebrafish embryos in the presence or absence of the chorion. *Environmental Toxicology and Chemistry*, *40*, 780–791. https://doi.org/10.1002/etc.4899

Newberry, E. P., Xie, Y., Kennedy, S., Han, X., Buhman, K. K., Luo, J., Gross, R. W., & Davidson, N. O. (2003). Decreased hepatic triglyceride accumulation and altered fatty acid uptake in mice with deletion of the liver fatty acid-binding protein gene. *The Journal of Biological Chemistry*, *278*, 51664–51672. https://doi.org/10.1074/jbc.M309377200

Nguyen-Lefebvre, A. T., & Horuzsko, A. (2015). Kupffer cell metabolism and function. *Journal of Enzymology and Metabolism*, *1*, 101.

Office of Chemical Safety and Pollution Prevention. (2015). *OCSPP 890.2200: Medaka Extended One Generation Reproduction Test (MEOGRT). Endocrine Disruptor Screening Program test guidelines*. U.S. Environmental Protection Agency. https://www.regulations.gov/document/EPA-HQ-OPPT-2009-0576-0019

Olivares-Rubio, H. F., & Vega-López, A. (2016). Fatty acid metabolism in fish species as a biomarker for environmental monitoring. *Environmental Pollution*, *218*, 297–312. https://doi.org/10.1016/j.envpol.2016.07.005

Oliveros, J. C. (2007). *VENNY: An interactive tool for comparing lists with Venn diagrams*. http://bioinfogp.cnb.csic.es/tools/venny/index.html

Patsouris, D., Reddy, J. K., Müller, M., & Kersten, S. (2006). Peroxisome proliferator–activated receptor α mediates the

effects of high-fat diet on hepatic gene expression. *Endocrinology*, *147*, 1508–1516. https://doi.org/10.1210/en.2005-1132

Pfohl, M., Ingram, L., Marques, E., Auclair, A., Barlock, B., Jamwal, R., Anderson, D., Cummings, B. S., & Slitt, A. L. (2020). Perfluorooctanesulfonic acid and perfluorohexanesulfonic acid alter the blood lipidome and the hepatic proteome in a murine model of diet-induced obesity. *Toxicological Sciences*, *178*, 311–324. https://doi.org/10.1093/toxsci/kfaa148

Pruitt, K. D., Brown, G. R., Hiatt, S. M., Thibaud-Nissen, F., Astashyn, A., Ermolaeva, O., Farrell, C. M., Hart, J., Landrum, M. J., McGarvey, K. M., Murphy, M. R., O'Leary, N. A., Pujar, S., Rajput, B., Rangwala, S. H., Riddick, L. D., Shkeda, A., Sun, H., Tamez, P., … Ostell, J. M. (2014). RefSeq: An update on mammalian reference sequences. *Nucleic Acids Research*, *42*, D756–D763. https://doi.org/10.1093/nar/gkt1114

Reddy, J. K. (2001). III. Peroxisomal β-oxidation, PPARα, and steatohepatitis. *American Journal of Physiology–Gastrointestinal and Liver Physiology*, *281*, G1333–G1339. https://doi.org/10.1152/ajpgi.2001.281.6.G1333

Roberts, L. D., Murray, A. J., Menassa, D., Ashmore, T., Nicholls, A. W., & Griffin, J. L. (2011). The contrasting roles of PPARδ and PPARγ in regulating the metabolic switch between oxidation and storage of fats in white adipose tissue. *Genome Biology*, *12*, R75. https://doi.org/10.1186/gb-2011-12-8-r75

Rodríguez-Jorquera, I. A., Colli-Dula, R. C., Kroll, K., Jayasinghe, B. S., Parachu Marco, M. V., Silva-Sanchez, C., Toor, G. S., & Denslow, N. D. (2019). Blood transcriptomics analysis of fish exposed to perfluoro alkyls substances: Assessment of a non-lethal sampling technique for advancing aquatic toxicology research. *Environmental Science & Technology*, *53*, 1441–1452. https://doi.org/10.1021/acs.est.8b03603

Rosen, M. B., Schmid, J. R., Corton, J. C., Zehr, R. D., Das, K. P., Abbott, B. D., & Lau, C. (2010). Gene expression profiling in wild-type and PPARα-null mice exposed to perfluorooctane sulfonate reveals PPARα-independent effects. *PPAR Research*, *2010*, 794739. https://doi.org/10.1155/2010/794739

Salter, D. M., Wei, W., Nahar, P. P., Marques, E., & Slitt, A. L. (2021). Perfluorooctanesulfonic acid (PFOS) thwarts the beneficial effects of calorie restriction and metformin. *Toxicological Sciences*, *182*, 82–95. https://doi.org/10.1093/toxsci/kfab043

Sant, K. E., Annunziato, K., Conlin, S., Teicher, G., Chen, P., Venezia, O., Downes, G. B., Park, Y., & Timme-Laragy, A. R. (2021). Developmental exposures to perfluorooctanesulfonic acid (PFOS) impact embryonic nutrition, pancreatic morphology, and adiposity in the zebrafish, *Danio rerio*. *Environmental Pollution*, *275*, 116644. https://doi.org/10.1016/j.envpol.2021.116644

Sherman, B. T., Hao, M., Qiu, J., Jiao, X., Baseler, M. W., Lane, H. C., Imamichi, T., & Chang, W. (2022). DAVID: A web server for functional enrichment analysis and functional annotation of gene lists (2021 update). *Nucleic Acids Research*, *50*, W216–W221. https://doi.org/10.1093/nar/gkac194https://davidbioinformatics.nih.gov/

Society for Advancement of AOPs. (2023). *AOP 529: Xenobiotic binding to peroxisome proliferator–activated receptors (PPARs) causes dysregulation of lipid metabolism leading to liver steatosis*. https://aopwiki.org/aops/529

Sun, C., & Zhang, S. (2015). Immune-relevant and antioxidant activities of vitellogenin and yolk proteins in fish. *Nutrients*, *7*, 8818–8829. https://doi.org/10.3390/nu7105432

Sun, X., Xie, Y., Zhang, X., Song, J., & Wu, Y. (2023). Estimation of per- and polyfluorinated alkyl substance induction equivalency factors for humpback dolphins by transactivation potencies of peroxisome proliferator–activated receptors. *Environmental Science & Technology*, *57*, 3713–3721. https://doi.org/10.1021/acs.est.2c05044

Sunderland, E. M., Hu, X. C., Dassuncao, C., Tokranov, A. K., Wagner, C. C., & Allen, J. G. (2019). A review of the pathways of human exposure to poly- and perfluoroalkyl substances (PFASs) and present understanding of health effects. *Journal of Exposure Science & Environmental Epidemiology*, *29*, 131–147. https://doi.org/10.1038/s41370-018-0094-1

Tahri-Joutey, M., Andreoletti, P., Surapureddi, S., Nasser, B., Cherkaoui-Malki, M., & Latruffe, N. (2021). Mechanisms mediating the regulation of peroxisomal fatty acid beta-oxidation by PPARα. *International Journal of Molecular Sciences*, *22*, 8969. https://doi.org/10.3390/ijms22168969

Takacs, M. L., & Abbott, B. D. (2007). Activation of mouse and human peroxisome proliferator–activated receptors (α, β/δ, γ) by perfluorooctanoic acid and perfluorooctane sulfonate. *Toxicological Sciences*, *95*, 108–117. https://doi.org/10.1093/toxsci/kfl135

Takahashi, N., Yao, L., Kim, M., Sasako, H., Aoyagi, M., Shono, J., Tsuge, N., Goto, T., & Kawada, T. (2013). Dill seed extract improves abnormalities in lipid metabolism through peroxisome proliferator–activated receptor-α (PPAR-α) activation in diabetic obese mice. *Molecular Nutrition & Food Research*, *57*, 1295–1299. https://doi.org/10.1002/mnfr.201200767

Tsai, T. H., Chen, E., Li, L., Saha, P., Lee, H. J., Huang, L. S., Shelness, G. S., Chan, L., & Chang, B. H. J. (2017). The constitutive lipid droplet protein PLIN2 regulates autophagy in liver. *Autophagy*, *13*, 1130–1144. https://doi.org/10.1080/15548627.2017.1319544

Tse, W. K. F., Li, J. W., Tse, A. C. K., Chan, T. F., Ho, J. C. H., Wu, R. S. S., Wong, C. K. C., & Lai, K. P. (2016). Fatty liver disease induced by perfluorooctane sulfonate: Novel insight from transcriptome analysis. *Chemosphere*, *159*, 166–177.

Tu, W., Martínez, R., Navarro-Martin, L., Kostyniuk, D. J., Hum, C., Huang, J., Deng, M., Jin, Y., Chan, H. M., & Mennigen, J. A. (2019). Bioconcentration and metabolic effects of emerging PFOS alternatives in developing zebrafish. *Environmental Science & Technology*, *53*, 13427–13439. https://doi.org/10.1021/acs.est.9b03820

Vanden Heuvel, J. P., Thompson, J. T., Frame, S. R., & Gillies, P. J. (2006). Differential activation of nuclear receptors by perfluorinated fatty acid analogs and natural fatty acids: A comparison of human, mouse, and rat peroxisome proliferator–activated receptor-α, -β, and -γ, liver X receptor-β, and retinoid X receptor-α. *Toxicological Sciences*, *92*, 476–489. https://doi.org/10.1093/toxsci/kfl014

Varga, T., Czimmerer, Z., & Nagy, L. (2011). PPARs are a unique set of fatty acid regulated transcription factors controlling both lipid metabolism and inflammation. *Biochimica et Biophysica Acta*, *1812*, 1007–1022. https://doi.org/10.1016/j.bbadis.2011.02.014

Varga, Z. M., & Murray, K. N. (2016). Health monitoring and disease prevention at the Zebrafish International Resource Center. *Methods in Cell Biology*, *135*, 535–551. https://doi.org/10.1016/bs.mcb.2016.04.020.

Venezia, O., Islam, S., Cho, C., Timme-Laragy, A. R., & Sant, K. E. (2021). Modulation of PPAR signaling disrupts pancreas development in the zebrafish, *Danio rerio*. *Toxicology and Applied Pharmacology*, *426*, 115653. https://doi.org/10.1016/j.taap.2021.115653

Villeneuve, D., Meek, B., Viviani, B., Burgdorf, T., LaLone, C., O'Brien, J., Knapen, D., Angrish, M., FitzGerald, R., Tanabe, S., & Karschnik, T. (2023). *Developers' handbook 2.6*. https://aopwiki.org/handbooks/4

Vujic, E., Ferguson, S. S., & Brouwer, K. L. (2024). Effects of PFAS on human liver transporters: Implications for health outcomes. *Toxicological Sciences*, *200*, 213–227. https://doi.org/10.1093/toxsci/kfae061

Wan, H. T., Zhao, Y. G., Wei, X., Hui, K. Y., Giesy, J. P., & Wong, C. K. (2012). PFOS-induced hepatic steatosis, the mechanistic actions on β-oxidation and lipid transport. *Biochimica et Biophysica Acta*, *1820*, 1092–1101. https://doi.org/10.1016/j.bbagen.2012.03.010

Wang, L., Wang, Y., Liang, Y., Li, J., Liu, Y., Zhang, J., Zhang, A., Fu, J., & Jiang, G. (2014). PFOS induced lipid metabolism disturbances in BALB/c mice through inhibition of low density lipoproteins excretion. *Scientific Reports*, *4*, 4582. https://doi.org/10.1038/srep04582

Wang, P., Liu, D., Yan, S., Cui, J., Liang, Y., & Ren, S. (2022). Adverse effects of perfluorooctane sulfonate on the liver and relevant mechanisms. *Toxics*, *10*, 265. https://doi.org/10.3390/toxics10050265

Wang, Q., Huang, J., Liu, S., Wang, C., Jin, Y., Lai, H., & Tu, W. (2022). Aberrant hepatic lipid metabolism associated with gut microbiota dysbiosis triggers hepatotoxicity of novel PFOS alternatives in adult zebrafish. *Environment International*, *166*, 107351. https://doi.org/10.1016/j.envint.2022.107351

Wang, Y., Nakajima, T., Gonzalez, F. J., & Tanaka, N. (2020). PPARs as metabolic regulators in the liver: Lessons from liver-specific PPAR-null mice. *International Journal of Molecular Sciences*, *21*, 2061. https://doi.org/10.3390/ijms21062061

Wang, Y. X., Lee, C. H., Tiep, S., Ruth, T. Y., Ham, J., Kang, H., & Evans, R. M. (2003). Peroxisome-proliferator-activated receptor δ activates fat metabolism to prevent obesity. *Cell*, *113*, 159–170. https://doi.org/10.1016/s0092-8674(03)00269-1

Watanabe, M., Houten, S. M., Wang, L., Moschetta, A., Mangelsdorf, D. J., Heyman, R. A., Moore, D. D., & Auwerx, J. (2004). Bile acids lower triglyceride levels via a pathway involving FXR, SHP, and SREBP-1c. *The Journal of Clinical Investigation*, *113*, 1408–1418. https://doi.org/10.1172/JCI21025

Widhalm, R., Granitzer, S., Natha, B., Zoboli, O., Derx, J., Zeisler, H., Salzer, H., Weiss, S., Schmitner, N., Kimmel, R. A., Österreicher, T., Oberle, R., Hengstschläger, M., Distel, M., & Gundacker, C. (2025). Perfluorodecanoic acid (PFDA) increases oxidative stress through inhibition of mitochondrial β-oxidation. *Environmental Pollution*, *367*, 125595. https://doi.org/10.1016/j.envpol.2024.125595

Wilson, C. G., Tran, J. L., Erion, D. M., Vera, N. B., Febbraio, M., & Weiss, E. J. (2016). Hepatocyte-specific disruption of CD36 attenuates fatty liver and improves insulin sensitivity in HFD-fed mice. *Endocrinology*, *157*, 570–585. https://doi.org/10.1210/en.2015-1866

Wolf, C. J., Takacs, M. L., Schmid, J. E., Lau, C., & Abbott, B. D. (2008). Activation of mouse and human peroxisome proliferator–activated receptor alpha by perfluoroalkyl acids of different functional groups and chain lengths. *Toxicological Sciences*, *106*, 162–171. https://doi.org/10.1093/toxsci/kfn166

Woolsey, S. J., Mansell, S. E., Kim, R. B., Tirona, R. G., & Beaton, M. D. (2015). CYP3A activity and expression in nonalcoholic fatty liver disease. *Drug Metabolism and Disposition: The Biological Fate of Chemicals*, *43*, 1484–1490. https://doi.org/10.1124/dmd.115.065979

Xie, C., Woollett, L. A., Turley, S. D., & Dietschy, J. M. (2002). Fatty acids differentially regulate hepatic cholesteryl ester formation and incorporation into lipoproteins in the liver of the mouse. *Journal of Lipid Research*, *43*, 1508–1519. https://doi.org/10.1194/jlr.m200146-jlr200

Xu, B., Chen, L., Zhan, Y., Marquez, K. N. S., Zhuo, L., Qi, S., Zhu, J., He, Y., Chen, X., Zhang, H., Shen, Y., Chen, G., Gu, J., Guo, Y., Liu, S., & Xie, T. (2022). The biological functions and regulatory mechanisms of fatty acid binding protein 5 in various diseases. *Frontiers in Cell and Developmental Biology*, *10*, 857919. https://doi.org/10.3389/fcell.2022.857919

Yan, S. (2022). Role of TFEB in autophagy and the pathogenesis of liver diseases. *Biomolecules*, *12*, 672. https://doi.org/10.3390/biom12050672

Yi, S., Chen, P., Yang, L., & Zhu, L. (2019). Probing the hepatotoxicity mechanisms of novel chlorinated polyfluoroalkyl sulfonates to zebrafish larvae: Implication of structural specificity. *Environment International*, *133*, 105262. https://doi.org/10.1016/j.envint.2019.105262

Yilmaz, O., Patinote, A., Nguyen, T., Com, E., Pineau, C., & Bobe, J. (2019). Genome editing reveals reproductive and developmental dependencies on specific types of vitellogenin in zebrafish (*Danio rerio*). *Molecular Reproduction and Development*, *86*, 1168–1188. https://doi.org/10.1002/mrd.23231

Yu, S., Matsusue, K., Kashireddy, P., Cao, W. Q., Yeldandi, V., Yeldandi, A. V., Rao, M. S., Gonzalez, F. J., & Reddy, J. K. (2003). Adipocyte-specific gene expression and adipogenic steatosis in the mouse liver due to peroxisome proliferator--activated receptor γ1 (PPARγ1) overexpression. *The Journal of Biological Chemistry*, *278*, 498–505. https://doi.org/10.1074/jbc.M210062200

Zhang, L., Krishnan, P., Ehresman, D. J., Smith, P. B., Dutta, M., Bagley, B. D., Chang, S. C., Butenhoff, J. L., Patterson, A. D., & Peters, J. M. (2016). Perfluorooctane sulfonate-choline ion pair formation: A potential mechanism modulating hepatic steatosis and oxidative stress in mice. *Toxicological Sciences*, *153*, 186–197. https://doi.org/10.1093/toxsci/kfw120

Zhang, R., Yu, G., Luo, T., Zeng, X., Sun, Y., Huang, B., Liu, Y., & Zhang, J. (2024). Transcriptomic and metabolomic profile changes in the liver of Sprague Dawley rat offspring after maternal PFOS exposure during gestation and lactation. *Ecotoxicology and Environmental Safety*, *270*, 115862. https://doi.org/10.1016/j.ecoenv.2023.115862

Zhang, S., Peng, X., Yang, S., Li, X., Huang, M., Wei, S., Liu, J., He, G., Zheng, H., Yang, L., Li, H., & Fan, Q. (2022). The regulation, function, and role of lipophagy, a form of selective autophagy, in metabolic disorders. *Cell Death & Disease*, *13*, 132. https://doi.org/10.1038/s41419-022-04593-3

Zhang, W., Tian, Y., Chen, B., Xu, S., & Wu, L. (2024). PFOA/PFOS facilitated intestinal fatty acid absorption by activating the PPARα pathway: Insights from organoids model. *Environment & Health*, *2*, 85–94. https://doi.org/10.1021/envhealth.3c00129

Environmental Toxicology and Chemistry, 2026, 00, 1–25
https://doi.org/10.1093/etojnl/vgag143
Original Article Environmental Toxicology